Durability Aspects of Precast Prestressed Concrete — Parts 1 and 2*

by Matthew R. Sherman, David B. McDonald and Donald W. Pfeifer

Comments by Rachel J. Detwiler, David A. Whiting, and John W. Gajda, Per Fidjestøl, R. D. Hooton and Authors

RACHEL J. DETWILER,† DAVID A. WHITING‡ and JOHN W. GAJDA§

In calculating the times-to-corrosion for the various concretes, the authors have used Fick's Second Law of Diffusion to analyze the chloride profiles from cores taken from concrete slabs subjected to 12 months of ponding with NaCl solution. Fick's Second Law is frequently used for this purpose, but it is worth examining the assumptions on which it is based before applying the equation.

Pettersson[1] provides an excellent discussion of chloride ion transport in concrete, which can be summarized as follows. The general equation describing ion transport driven by a concentration gradient is:

$$\frac{\partial C}{\partial t} = \frac{\partial}{\partial x}\left(D\frac{\partial C}{\partial x}\right)$$

The chloride ion concentration C varies with both time t and location (distance from the surface) x, while the diffusion coefficient D is a function of x, t, and C. Fick's Second Law makes the simplifying assumption that D can be taken as a constant, D_0. Thus, the expression known as Fick's Second Law is:

$$\frac{\partial C}{\partial t} = D_0\frac{\partial^2 C}{\partial x^2}$$

Several conditions must be satisfied in order for the diffusion coefficient to be constant:

1. The material in which diffusion takes place must be permeable and homogeneous. The presence of interconnected pores, cracks, microcracks, and aggregate particles will affect the ability of the chloride ions to migrate into the concrete.
2. The diffusion properties of concrete in most practical cases will certainly change with time as hydration proceeds. They may also be affected by the chloride ion concentration.
3. The hydration products of the aluminates in the cement and/or supplementary cementing materials bind chlorides.

In addition, there is more than one mechanism of chloride ion transport through concrete in a ponding test. Capillary action undoubtedly plays a much more significant role near the concrete surface when the concrete has been allowed to dry out, as is the case in AASHTO T259. Pettersson reports that for a 0.40 water-cement (w/c) ratio concrete dried at room temperature and 60 percent relative humidity, the effect of capillary action was at least twenty times as great as that of diffusion.

At this point, the question naturally arises as to how applicable Fick's Second Law is. Fig. A is a plot of chloride concentration vs. distance from the surface for a 0.40 w/c ratio concrete subjected to 6 months of ponding with 3 percent NaCl under the conditions described by AASHTO T259. A 100 mm (4 in.) diameter core was milled in layers to produce separate samples, each representing approximately 1 mm (0.039 in.) of thickness, in order to obtain the data points.

The curve is the best fit of Fick's Second Law as determined by a curve-fitting program; the apparent diffusion co-

* PCI JOURNAL, V. 41, No. 4, July-August 1996, pp. 62-95.
† Principal Engineer, Construction Technology Laboratories, Inc., Skokie, Illinois.
‡ Senior Principal Scientist, Construction Technology Laboratories, Inc., Skokie, Illinois.
§ Engineer, Construction Technology Laboratories, Inc., Skokie, Illinois.

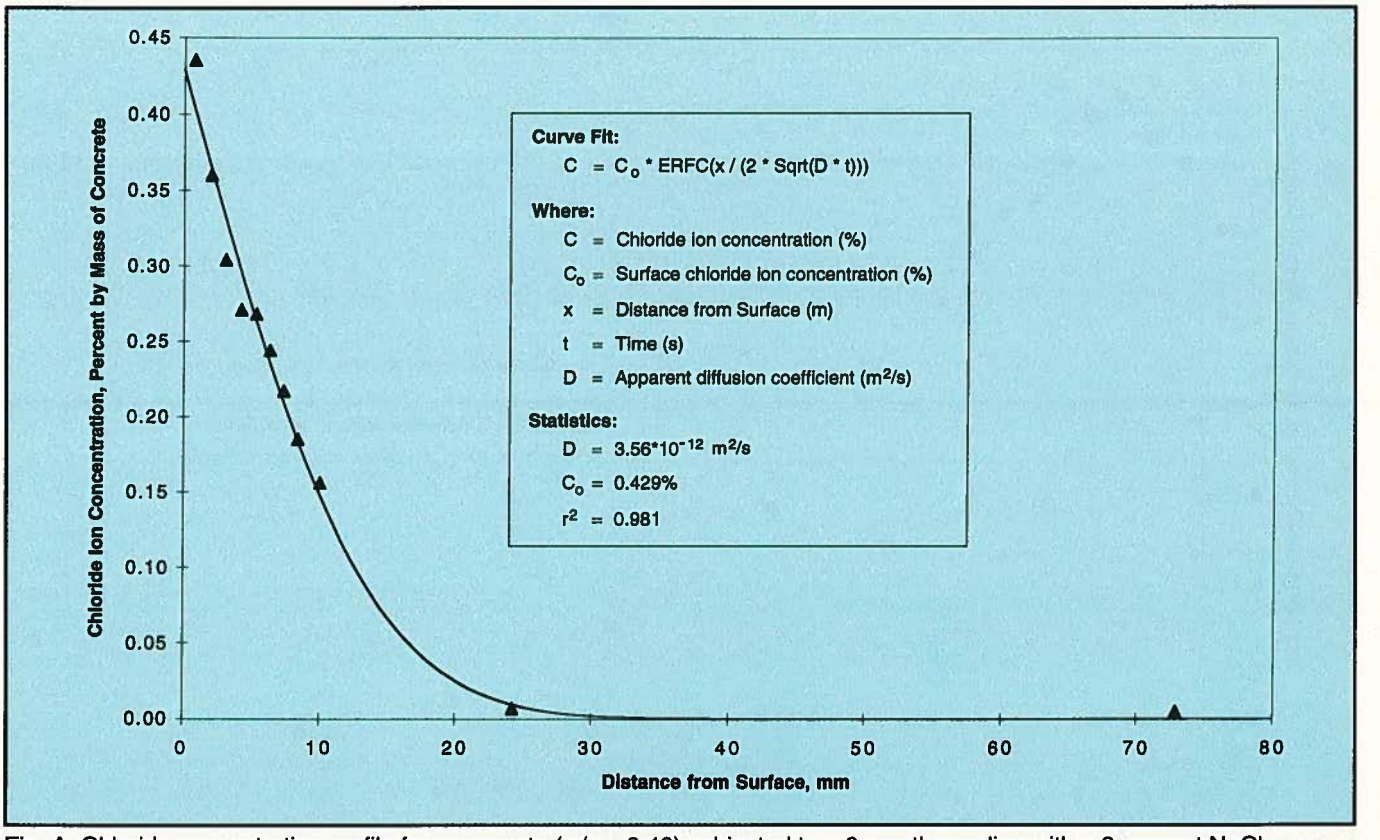

Fig. A. Chloride concentration profile for a concrete (w/c = 0.40) subjected to a 6 month ponding with a 3 percent NaCl solution. The curve is the best fit of Fick's Second Law of Diffusion. Note that the fit is excellent even though the dominant transport mechanism is capillary action.

efficient is 3.56×10^{-12} m²/sec and the chloride concentration at the surface is projected to be 0.429 percent by mass of concrete. Thus, even though all three of the assumptions of Fick's Second Law have been violated and the dominant mechanism of transport, at least in the first 10 mm (0.39 in.) or so from the surface, is capillary action rather than diffusion, the equation does yield a curve that can be fitted to the data.

In moving from the laboratory to the field, further deviations from the conditions of Fick's Second Law are introduced. In the laboratory, the temperature is close to constant, while in the field the temperature fluctuates both daily and seasonally. All transport mechanisms are slower at lower temperatures and if the temperature is low enough to freeze the pore solution, the phase change from liquid to solid will reduce the rate of transport far more than the simple effect of temperature. That is, the rate of diffusion in ice will be much slower than in the liquid pore solution.

In the laboratory, the continuous ponding of the concrete with a solution of more or less constant concentration provides a consistent driving force for chloride ion transport in one direction. In the field, there are cycles of wetting and drying. Wetting washes out some chlorides from the surface, a mechanism of reverse migration, while drying concentrates the chloride ions in the pore solution. There may also be other ions present which affect the rate of chloride ion transport.

The combination of some of these effects can be seen in Fig. B (adapted from Detwiler et al.[2]), which shows chloride profiles obtained as described above for cores taken from a bridge deck approximately 8 years after replacement of the concrete. The reduced concentration of chloride ions at the surface, as compared to several millimeters from the surface, illustrates the effects of cycles of wetting and drying. The shape of these profiles suggests that Fick's Second Law may not be appropriate for prediction of chloride ion transport in this type of field exposure.

Pettersson reports a comparison of effective diffusion coefficients determined for concretes under laboratory conditions with similar values determined for concretes exposed to a marine environment. The effective diffusion coefficients for the field concretes were an order of magnitude lower. She attributes this difference to a combination of the effects of temperature (much lower outdoors than in the laboratory), the continuing hydration of the cement over time, and the presence of other ions in seawater that would compete with the chloride ions.

It is clear from the preceding discussion that the use of diffusion coefficients derived from the ponding test (AASHTO T259) is not appropriate for the purpose of predicting the service life of concrete in the field. The determination of an apparent diffusion coefficient by applying Fick's Second Law to the data is convenient because it provides a single number with which to rate different concretes.

The "goodness of fit" of the curve to the data may suggest that the equation is a good model of the behavior, but a careful examination of the mechanisms of transport under labo-

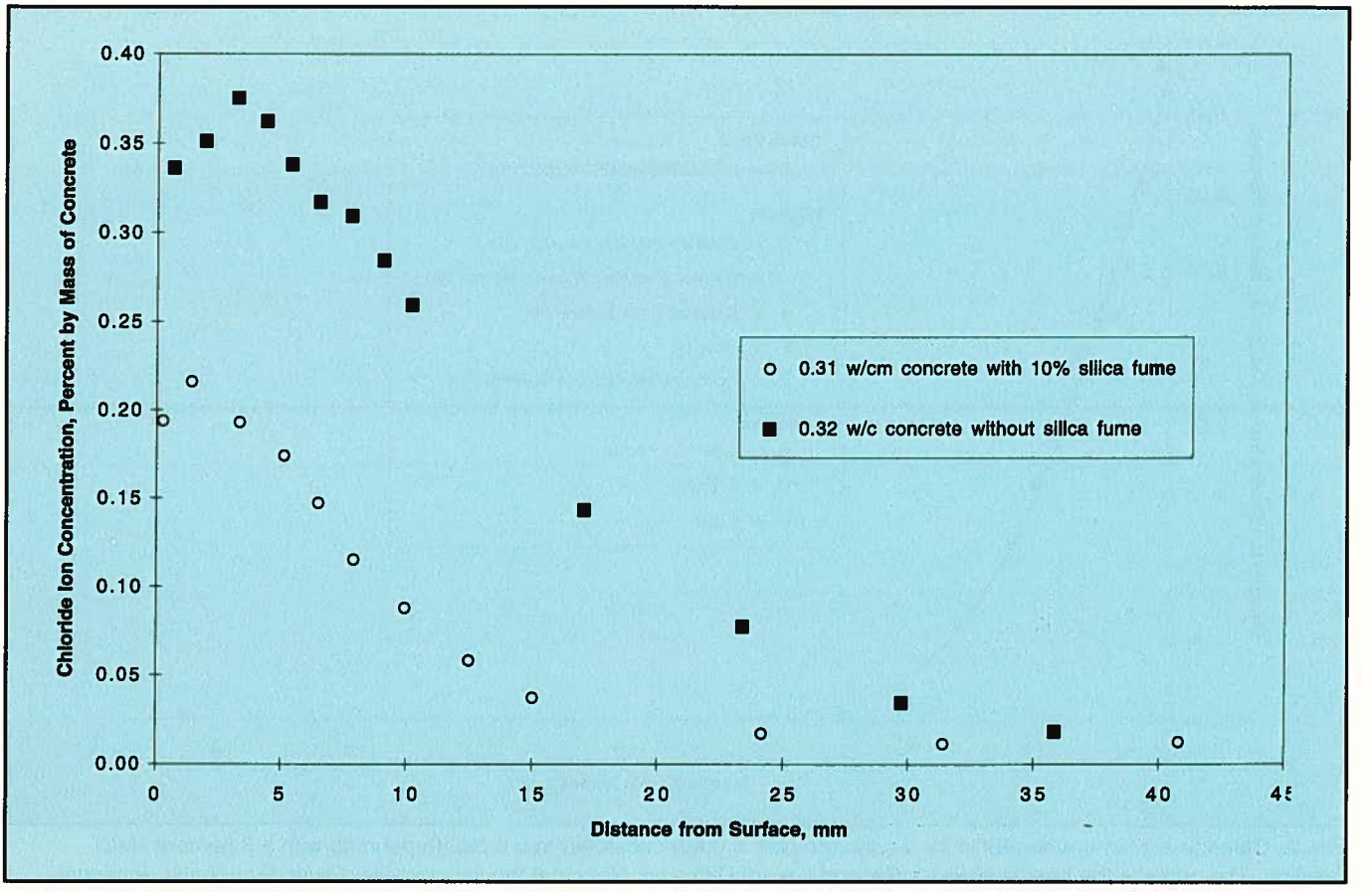

Fig. B. Chloride concentration profile obtained from an 8-year-old bridge deck (adapted from Detwiler et al.[8]). In this case, additional transport mechanisms such as washout change the shape of the profile so that the equation for Fick's Second Law does not fit the data.

ratory and field conditions indicates that caution is necessary in making any predictions. We recommend that the ponding test be used only for comparative purposes. Provided that the conditions for all concretes tested are the same, the comparison is valid, even though the use of Fick's Second Law is not. It is helpful to use a term such as "apparent diffusion coefficient" to make clear that what has been determined is not strictly a diffusion coefficient and should not be used as if it were.

We agree with the authors that some modifications to the test method may be appropriate for use with high quality concretes. For example, increasing the ponding period to 6 months allows more time for the chloride ions to migrate into the concrete. Increasing the number of samples provides more data and greater confidence in the apparent diffusion coefficients calculated from them. The increased number of data points allows for a "reasonableness" check of any given data point, as under these test conditions the chloride concentration should consistently decrease with distance from the surface. The sample sizes are sufficient to allow retesting of any suspect points. The use of core samples allows one to maintain the integrity of the sample; however, 100 mm (4 in.) diameter cores are necessary to provide representative samples when milling of thin layers is employed. A higher chloride concentration in the ponding solution is unnecessary, as the detection limits for titration are about 20 to 30 ppm (0.002 to 0.003 percent).

In summary, Fick's Second Law of Diffusion must be used with caution in analyzing data from the ponding test (AASHTO T259), as all of the assumptions on which it is based are violated, even under the controlled conditions of the laboratory. In addition, the dominant mechanism of chloride ion transport near the surface of the concrete is not diffusion, but capillary action.

Field conditions deviate even further from the conditions assumed for Fick's Law. The transport mechanisms for chloride ions under these conditions include washout and concentration due to drying as well as diffusion and capillary action. Thus, it is not appropriate to use Fick's Law to predict the service life of concrete in the field. Fick's Law can be used to compare the performance of different concretes subjected to the same conditions in the laboratory. If greater precision and/or confidence in the data are desired, the concrete can be sampled by milling thin layers from a 100 mm (4 in.) diameter core. However, even these more precise data cannot predict the service life of concrete in the field.

REFERENCES

1. Pettersson, Karin, "The Effect of Different Factors on the Chloride Diffusion in Concrete," CBI Report 4:94, Cement och Betong Institutet, Stockholm, Sweden, 1994, 37 pp. (in Swedish).
2. Detwiler, Rachel J., Kojundic, Tony, and Fidjestøl, Per, "Evaluation of Staunton, Illinois, Bridge Deck Overlays." (To be published in the August 1997 issue of *Concrete International.*)

PER FIDJESTØL*

Over the years, as a provider of microsilica to the concrete industry, we have often been presented with valid technical concerns from our clients, which have been resolved to the best of our abilities. With time, the value of microsilica in the production of quality concrete has come to be recognized by the industry. Particularly in the prestressed concrete industry, the industrial setting is a great opportunity for realizing the potential of new developments in concrete technology.

Moving on to the paper in the July-August issue of the PCI JOURNAL on chloride permeability, it breaks new ground in that it provides a number of new experiences and insights that are contrary to most of the accumulated technical expertise available. I am surprised that a warning bell did not ring in the technical offices of WJE and PCI when they looked at the 28-day strength results. Fig. C plots these strength results for burlap-cured specimens against water-cement (w/c) ratio.

Fig. C shows that there is a serious problem with the silica fume mixes used in the study. All experience shows that replacing cement with equal amounts of silica fume produces an increase in strength (e.g., Fig. D from Sellevold and Radjy, 1983[3]).

In our experience, the data in the figure indicate very poor and uneven dispersion of the silica fume. From a large volume of experience, it is well known that if using Duff Abram's Law, silica fume can replace cement with a factor of about 3 (depending on cement and mix design). The erratic behavior of the w/c-strength plot is a clear indicator that the mixes with silica fume were improperly made. In the case of the water-cementitious materials (w/cm) = 0.46 mix, the evidence of the strength tests is that only one-third of the silica fume was properly dispersed; the remainder existed as agglomerates throughout the mix and did not provide the property improvements that silica fume is supposed to provide.

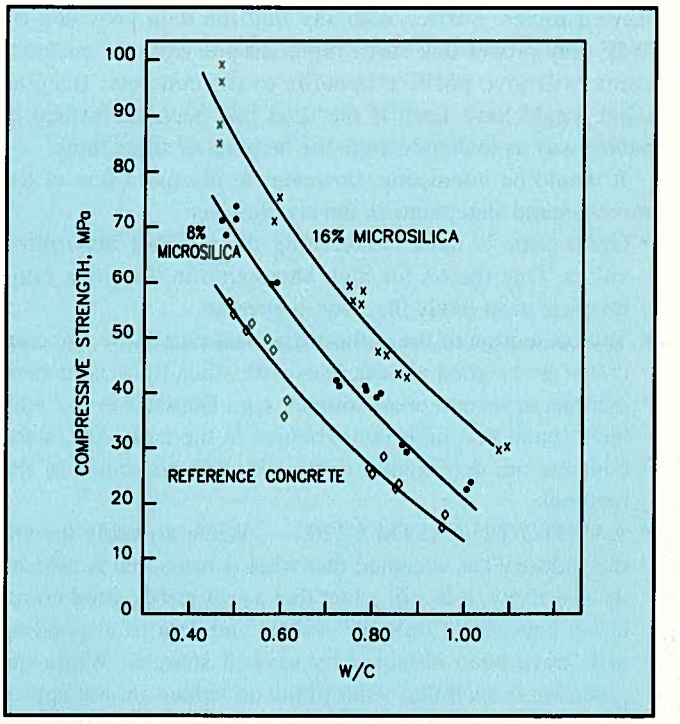

Fig. D. Typical results for strength of concrete with varying silica fume content vs. water-cement ratio (from Sellevold and Radjy, 1983[3]).

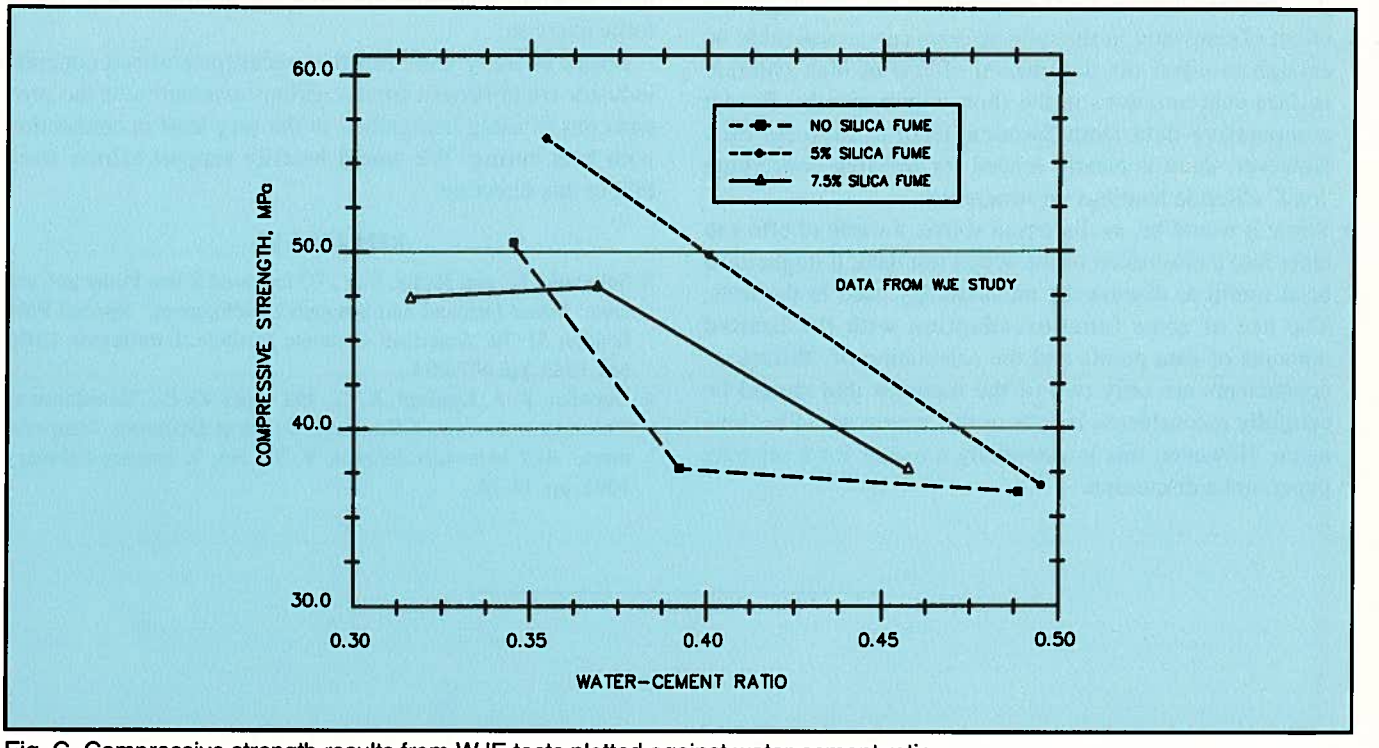

Fig. C. Compressive strength results from WJE tests plotted against water-cement ratio.

* Technical Manager, Elkem Materials Inc., Kristiansand, Norway.

From the above, it is clear that it does not make sense to go into a critical review of data that are obviously based on flawed mixes. Suffice it to say that the data provided by WJE only proves that silica fume, despite extreme mistreatment, will give positive benefits to the concrete. Imagine what would have been if the tests had been performed in such a way as to demonstrate the benefits of silica fume.

It would be interesting, however, to discuss a few of the more general statements in the conclusions:

- Great issue is made concerning the variable absorption values. One reason for high absorption in the silica fume mixes is most likely the poor dispersion.
- The contention of the authors that heat-cured low w/c concretes are as good as concretes with silica fume is in stark contrast to several other sources, e.g., Detwiler et al.,[4] who have found that high temperatures in the early life of the concrete are detrimental to the chloride resistance of the material.
- AASHTO T277/ASTM C1202 — While arguably the entire industry has accepted that what is measured is primarily resistivity, it is still a fact that a reasonably good correlation between "Coulomb" values and data from ponding tests have been obtained by several sources. While the precision is such that strict limits on values are not appropriate, the method nevertheless is useful in a qualitative and qualified comparison of concrete mixtures.
- AASHTO T259 — Realistic curing period. The age of the specimen at the time of testing and the amount of moist curing it receives is definitely a subject for discussion. Very often, 7 days of moist curing is the absolute maximum that can be expected. However, very few concretes will be exposed to salt at 28 days; thus, a high age of concrete before exposure should be considered.
- AASHTO T259 — Chloride concentration. It is not certain that de-icing conditions are the most severe. Even if the concentrations in the winter season are very high, the effect of rainwater in the mild seasons can conceivably be enough to offset the detrimental effects of high chloride surface concentrations in the short winter months. Recent comparative data from Sweden seem to indicate this. However, there is clearly a need for research concerning "real" chloride loadings on structures.
- While it would be, as discussed above, a waste of effort to enter into a discussion of the actual test data, it might have been useful to discuss the methodology used in the tests. The use of error function adaption with the limited amounts of data points and the calculation of "diffusion" coefficients are only two of the methods that should be carefully reconsidered if tests of this nature are to be done again. However, this is essentially a matter for a separate paper, not a discussion.
- If the data, and especially the conclusions, from the report are used without careful evaluation, the risk of selecting a non-optimal concrete mixture is real.

In conclusion, the judicious use of microsilica will provide:

1. High early strength — Because microsilica is a very efficient pozzolan, combination with accelerated curing through temperature elevation will give a very rapid strength gain. This is useful for purposes of form stripping, release of tendons, and other factors. In England, more than 110 MPa (16,000 psi) was obtained at room temperature after 24 hours.

2. Prevention of deleterious effects of high temperature curing — The WJE study is interesting in that it contradicts most studies on the effects of high temperature curing on chloride permeability that are available. Most other studies show that microsilica will prevent the microstructure degradation normally expected from curing at high temperatures. This means that increases in chloride permeability and decreases in concrete strength normally associated with high temperature curing will be made less serious through the use of silica fume. It is a regrettable omission that heat-cured microsilica concrete was not included in the test program.

3. Delayed ettringite formation (DEF) is a real concern in the precast industry. An increasing amount of evidence seems to show that at high temperature curing, DEF can be a real concern. Scandinavian research appears to show that microsilica will eliminate — or at least strongly reduce — this problem.

In summary, this discussion started out as a critique of the WJE paper. However, after analyzing the data, it was apparent that the data were not appropriate for showing the benefits of silica fume concrete, as exemplified in the strength results. Thus, it is felt that because the data and test design were flawed, an attempt to discuss the detailed results was a futile exercise.

Elkem strongly feels that the precast/prestressed concrete industry could benefit from a serious evaluation of the pros and cons of using microsilica, at the very least in connection with heat curing. We would heartily support efforts from PCI in this direction.

REFERENCES

3. Sellevold, E., and Radjy, F. F., "Condensed Silica Fume in Concrete: Water Demand and Strength Development," Special Publication SP-79, American Concrete Institute, Farmington Hills, MI, 1983, pp. 677-694.
4. Detwiler, R. J., Kjellsen, K. O., and Gjorv, O. E., "Resistance to Chloride Intrusion of Concrete Cured at Different Temperatures," *ACI Materials Journal*, V. 88, No. 1, January-February 1991, pp. 18-24.

R. D. HOOTON*

Although the authors have performed an extensive test program, their conclusions appear to be far stronger than their experimental design and data suggest. I do not have the space to discuss this extensively, but will focus on a few points.

PART 1

In their historical review, the authors curiously ignored the publications of R. Detwiler. Ref. 5 shows that despite proper preset times, chloride diffusion coefficients, especially those of portland cement concretes, were significantly higher when exposed to steam curing. Also, this increase in chloride diffusion was indicated by the ASTM C1202 rapid test.

PART 2

1. In Table 1, it can be seen that although the authors kept the water-cementitious materials (w/cm) contents of their concrete mixtures approximately the same for comparison of 0, 5 and 7.5 percent silica fume replacements, they did not maintain a constant water content. By their own admission, the water contents were deliberately increased from 149 to 159 to 164 liters/m^3 with increasing silica fume content. While constant w/cm ratios should yield similar compressive strengths as per Abram's law, the unit water content of a mixture sets its initial porosity and is far more important in influencing both its permeability[6,7] and diffusion properties.

Based on the data in Ref. 6, a 10 percent increase in unit water content, as was done here, would increase water permeability by up to four times. Therefore, the authors appear to have deliberately or otherwise produced concretes that would put the silica fume concretes at a disadvantage for the chloride penetration tests they carried out. In fact, this fundamental difference makes all of their conclusions suspect.

The authors comment on this by stating that "the additional water was required to maintain the w/cm ratio with the added silica fume materials." This is curious because with appropriate high range water reducers, workable non-segregating concretes can be obtained with lower water contents when silica fume is used — both in the laboratory and in industry. In Toronto, flowing silica fume concretes with w/cm = 0.32 to 0.37 are typically placed on site with only 135 to 145 kg/m^3 of water.

2. The authors have used the AASHTO T259 chloride ponding test extensively. Unfortunately, the sampling procedures used in this test method and those used in this study are too crude to give much useful information about relative chloride penetration resistance of concretes. This is evidenced in Fig. 4 where, for the 0.32 w/cm concretes, no significant chloride concentration was measured at the 0.7 in. (17.8 mm) depth. Surface chloride differences [at 0.1 in. (2.5 mm) depth] have little bearing on long-term penetration resistance and could be due to several things including chloride binding effects or, as the authors suggest, where absorption dominates.

The improved chloride penetration resistance of the silica fume concretes shows up in Fig. 3 (0.37 w/cm) as these were the only sets of data with no significant chloride penetration at a 0.7 in. (17.8 mm) depth.

3. The authors have chosen to fit diffusion coefficients to

* Professor, Department of Civil Engineering, University of Toronto, Toronto, Ontario, Canada.

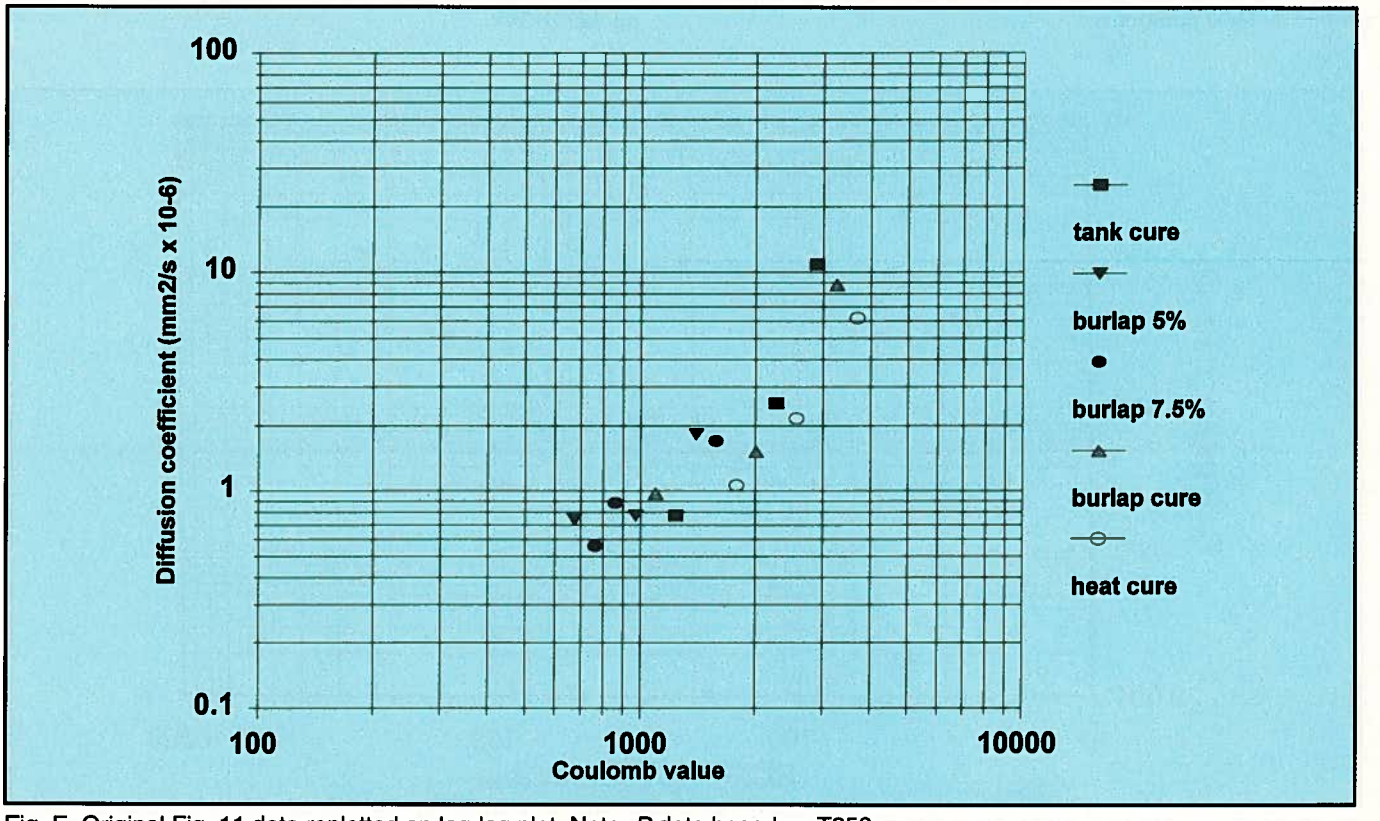

Fig. E. Original Fig. 11 data replotted on log-log plot. Note: *D* data based on T259.

their T259 chloride penetration profiles, but these cannot be considered diffusion values. In T259, the salt water solution is initially applied to partially dry concretes so a significant depth of penetration occurs by sorption, and the bottom of the slabs are exposed to 50 percent relative humidity during ponding, which induces a wicking action as well. My own tests indicate that in a standard AASHTO T259 90-day ponding test, up to one-third of the 90-day chlorides have penetrated after a few hours due to initial absorption and not diffusion. From a mechanistic viewpoint, this test procedure involves at least three mechanisms of chloride penetration and diffusion is not clearly the dominant mechanism at 90 days; however, in real structures over the long term, it will be.

4. The authors conclude (as part of Conclusion No. 9) that times-to-corrosion of 0.37 w/cm silica fume concretes are similar to those of heat-cured 0.37 to 0.32 w/cm plain concretes. This is in contrast to their data in Table 12 where times-to-corrosion of heat-cured 0.37 and 0.32 concretes are 14 and 20 years, respectively, while those of the 0.37 silica fume concretes are 25 years. This is hardly similar. I will not comment on the 0.46 concretes because the Canadian CSA A23.1 does not allow concretes of w/cm greater than 0.40 for severe exposures to chlorides, so in the Canadian context they have little relevance.

5. While the authors are critical of the AASHTO T259 test, they go on to criticize the ASTM C1202 rapid test because it does not agree with the results of their inappropriately calculated diffusion coefficients from the not-so-rigorous chloride ponding data. In Figs. 11 and 12, they plot a comparison of their diffusion coefficients with coulomb values on linear scales. Both the diffusion coefficients and the coulomb scales should be represented on logarithmic scales. It should be noted that 2000 coulombs is far more than twice as bad as 1000 coulombs.

In addition, the linear 10^{-6} mm^2/s scale in these figures makes little sense because values do not go to zero but go down to the range of 10^{-7} or 10^{-8} and beyond. If their data are replotted on a log-log scale, the relationship becomes much clearer (see Fig. E). In fact, from our data where effective diffusion coefficients calculated from steady state migration tests[8] are compared to the C1202 rapid test, we get a similar good relationship with data from a number of independent test programs, as shown in Fig. F.

Unfortunately, much of this data is as yet unpublished.

Based on our results, I believe that the ASTM C1202 rapid chloride test can be used with confidence to predict chloride diffusion rates, and I would certainly not recommend correlating it with the T259 chloride ponding test due to its own limitations.

REFERENCES

5. Detwiler, R. J., Fapohunda, C., and Natale, J., "Use of Supplementary Cementing Materials to Increase the Resistance to Chloride Ion Penetration of Concretes Cured at Elevated Temperatures," *ACI Materials Journal*, V. 91, No. 1, January-February 1994, pp. 63-66.
6. Hooton, R. D., "High Strength Concrete as a By-Product of Design for Low Permeability," Proceedings, V. 2, Concrete 2000, Dundee, Scotland, 1993, Chapman and Hall, R. K. Dhir and R. R. Jones, Editors, pp. 1627-1638.
7. Mills, R. H., "Mass Transfer of Gas and Water Through Concrete," Special Publication SP-100, *Concrete Durability*, V. 1, American Concrete Institute, Farmington Hills, MI, 1987, pp. 621-637.
8. McGrath, P. F., and Hooton, R. D., "Influence of Voltage on Chloride Diffusion Coefficients from Chloride Migration Tests," *Cement and Concrete Research*, V. 26, No. 8, 1996, pp. 1239-1244.

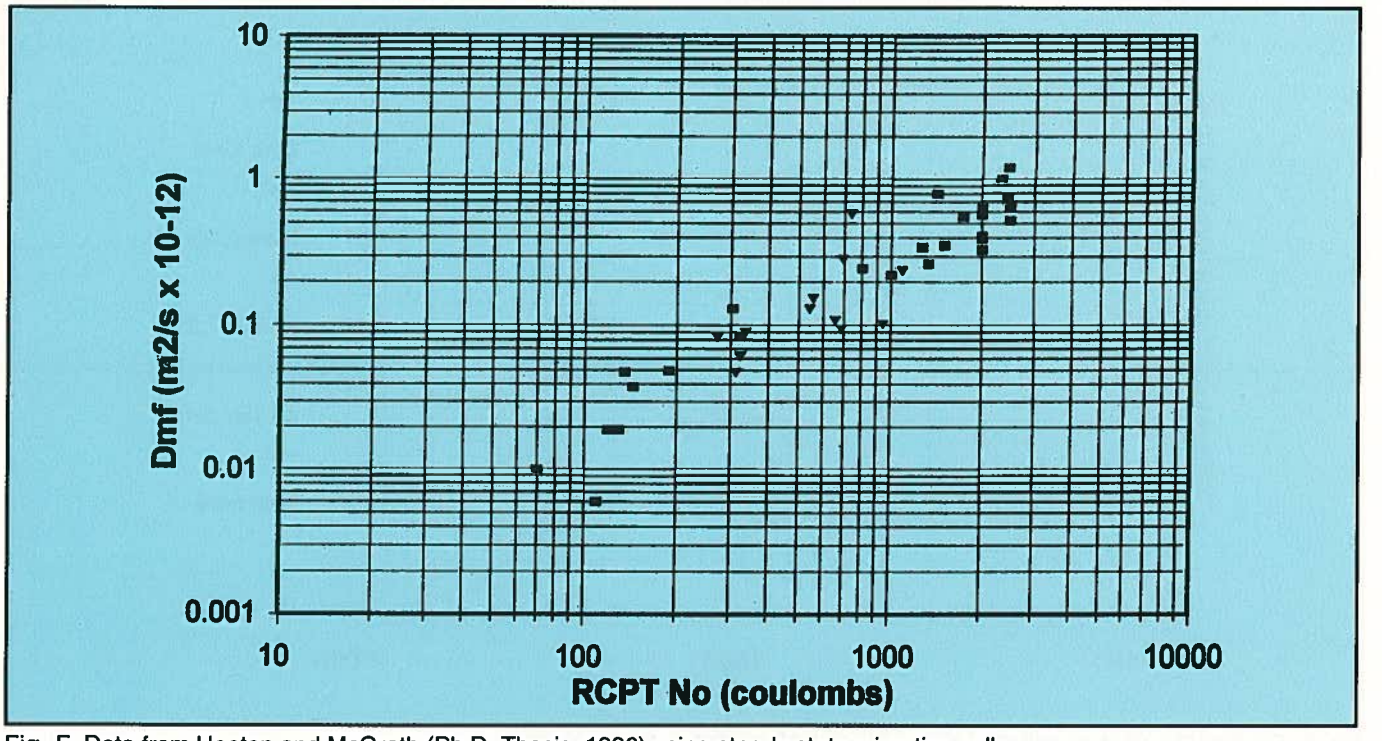

Fig. F. Data from Hooton and McGrath (Ph.D. Thesis, 1996) using steady state migration cells.

AUTHORS' CLOSURE by MATTHEW R. SHERMAN,* DAVID McDONALD† and DONALD W. PFEIFER‡

The authors welcome the discussions of Drs. Fidjestøl, Hooton, Detwiler and Whiting and Mr. Gajda.

Drs. Detwiler and Whiting and Mr. Gajda provide an excellent summary and discussion of the diffusion of chloride ions in concrete. They suggest many factors governing the diffusion of chloride ions in concrete including: non-homogeneity of the material, changes in diffusion coefficient with time, chemical reactions between the paste and the chloride ions, capillary action, variable temperatures, wetting and drying, reverse migration, continued hydration of the cement, and the effect of competing ions. We agree with this assessment; however, modeling of chloride ingress that considers all of these factors exceeds the current (and probably future) state-of-the-art in modeling.

We acknowledge that the transport of chloride in concrete follows a far more complicated mechanism than that described by simple Fick's Second Law diffusion. The simplifying assumption of Fick's Second Law diffusion and an effective diffusion coefficient does, however, provide a superior means of comparing the permeabilities of different concretes as compared to commonly used techniques such as "integral chloride" or depth-specific comparisons. The effective diffusion coefficient calculations are more representative because they take the approximate shape of the chloride distribution into account. In our paper, we briefly discussed some of the limitations of this method.

The calculation of "times-to-corrosion" of the different concretes presented in the paper was performed in order to allow those not familiar with diffusion calculations to better understand the results of the testing. As stated in the article, the comparisons were made using the simplifying assumptions of constant chloride at the concrete surface, linear diffusion constants, and constant temperature during the testing. We acknowledge that although these assumptions may be true for submerged or constantly ponded concrete, they may not be accurate for other field exposures. Despite these limitations, we consider that the effective diffusion constants are useful in the comparison of the various concrete mixtures.

We address Dr. Fidjestøl's comments as follows:

1. Effect of silica fume on strength — Dr. Fidjestøl presented data from Sellevold and Radjy showing that concretes with very high water-cementitious materials (w/cm) ratios together with 8 and 16 percent of silica fume exhibited an increase in compressive strength. This is not what was done during our recent PCI study. This current study included silica fume as an addition and not a replacement. The water content was increased to hold the w/cm ratio constant.

The concretes studied by Sellevold and Radjy were highly unusual, exhibiting extremely high compressive strengths of about 56 to 99 MPa (8100 to 14,500 psi) at w/cm ratios of about 0.47. The 0.47 w/cm ratio, air-entrained concretes examined in the current study produced 28-day compressive strengths of about 36 to 39 MPa (5200 to 5600 psi), showing no strength benefits from the fume.

The moist-cured 0.32 w/cm ratio concretes with 0, 5.0, and 7.5 percent fume additions produced an average 180-day strength of 62.4 MPa (9045 psi) with a low coefficient of variation of 3.2 percent, also indicating no beneficial strength increase due to either the 5.0 or 7.5 percent silica fume when at an equal w/cm ratio. It is quite clear that these concretes from our study cannot be directly compared with the unusual concretes by Sellevold and Radjy due to a number of significant factors, as clearly stated in our paper and in this response.

2. Was the silica fume properly dispersed? — Dr. Fidjestøl further states that the strength data indicate poor and uneven dispersion of the silica fume, speculating that up to two-thirds of the silica fume was improperly dispersed, existing as agglomerates in the mix. We strongly disagree with the assertions that the concrete used in the testing program was "flawed" and suffered "extreme mistreatment" for the following reasons:

First, the 28-day and 180-day compressive strength data from our study has been carefully reviewed and compared with other strength data from many other laboratory studies conducted by the authors using Wisconsin river gravel air-entrained and non-air-entrained concretes. This review finds the PCI compressive strength data in line and appropriate, except for the single 28-day strength [37.0 MPa (5370 psi)] from the 0.38 w/cm ratio, 5 percent silica fume mixture that exhibited lower than expected strength. However, this same concrete, when tested at 18 days, was in line with all the other moist-cured mixtures, indicating that the low 28-day strength is erroneous for some unknown reason and that the other 58 cylinder strengths out of 60 tests are appropriate and not flawed.

The 28-day strength data show the beneficial effects of silica fume at nominal 0.32 and 0.37 w/cm ratios. The strength increases were 17 percent for the 0.32 w/cm and 3 percent for the 0.37 w/cm for the 7.5 percent silica fume mixes, when compared on equal w/cm ratios.

In a 1993 paper by French and Mokhtarzadeh,[9] 28-day strength increased due to 7.5 percent silica fume replacement in moist-cured and heat-cured concretes ranged from 1 to 24 percent, averaging 9 percent with rounded gravel and crushed limestone, with the aggregate type playing a major role in the strength increase due to silica fume. Thus, the authors' data are in line with other studies.

Second, the counter rotating high-shear pan mixer used for the study is above the average used in the industry for concretes containing silica fume. Further, to aid in the mixing process and to eliminate health hazards, the silica fume was added as a slurry to the concrete. The fume necessary for each batch was first mixed in an equal weight of water with a high speed vane to ensure that a slurry was properly dispersed immediately prior to adding the silica fume slurry to the concrete.

After adding the silica fume, the concrete was mixed for a total of 5 minutes as required in ASTM C 192, *Standard*

* Project Engineer, Wiss, Janney, Elstner Associates, Inc., Northbrook, Illinois.
† Senior Engineer, Wiss, Janney, Elstner Associates, Inc., Northbrook, Illinois.
‡ Vice President, Wiss, Janney, Elstner Associates, Inc., Northbrook, Illinois.

Practice for Making and Curing Concrete Test Specimens in the Laboratory. This 5 minutes of vigorous pan mixing further dispersed and broke down any remaining densified material. These mixing techniques have been recommended to, and used by, the authors for many different clients, including clients who sell silica fume. If this mixing regime constitutes "extreme mistreatment" of the silica fume, as alleged, it is hard to imagine what extremely specialized equipment and techniques would be required in the ready-mixed or precast industries to properly mix concrete containing densified silica fume.

Thirdly, we have reviewed the mixture proportions, the batch data, the ASTM C 642 absorption after immersion and absorption after immersion and boiling data, the volume of permeable voids data, the AASHTO T 277 42-day coulomb data, the measured chloride contents, the calculated surface chloride concentrations, the calculated diffusion coefficients and the relationship between our calculated diffusion coefficients and our measured coulomb values shown in our Figs. 11 and 12 for the 15 different mixtures, as well as the other data, shown in Fig. 12 of our paper. All of these data are consistent with their w/cm ratios, their curing environments and their 28-day and 180-day compressive strengths, except for the single 28-day, 0.38 w/cm ratio concrete strength with 5.0 percent silica fume, discussed above.

Dr. Fidjestøl's discussion then continues, assuming that the mixtures are flawed. This position is impossible to support.

3. Contrast to Detwiler et al. (1991) — The paper by Detwiler et al.[10] used by Dr. Fidjestøl to support the conclusion that high temperature curing is detrimental to chloride resistance was extensively discussed by Perenchio.[11] Perenchio states:

> "The present study [by Detwiler et al.] which evaluated only one elevated curing temperature [122°F (50°C)], did not include a preset period, and in fact started with a concrete mixture temperature of 95°F (35°C)."

In the reply by Detwiler et al., it is stated that the concretes were pre-warmed and cured; thus, they represent a study of the hydration, strength, and permeability of hot concrete. Note that these are very different circumstances from our heat-cured samples: hot concrete sets and subsequently hydrates at an elevated temperature, while heat-cured concrete sets normally at room temperature until initial set (ASTM C 403) and is subsequently brought to a higher temperature to speed hydration after the initial set has taken place. The paper by Detwiler et al. was considered during the literature review for the current study; however, it was ruled inapplicable to the study of heat-cured concretes.

4. ASTM/AASHTO Tests — Dr. Fidjestøl states that relatively good correlations have been shown to exist for the AASHTO T 277/ASTM C 1202 test methods and permeability and that the test procedure essentially measures resistivity, and not chloride ingress. Problems with the coulomb tests are discussed in other papers by the authors and others[12-19] and the coulomb test procedure is receiving increasing worldwide criticism as being unable to accurately determine chloride penetration, as shown below.

Andrade[20] concludes that:

> "The rapid chloride permeability test (AASHTO), in its present formulation, cannot inform on concrete permeability to chlorides."

Arup, Sorenson, Frederiksen and Thaulow[21] concluded from a study of the AASHTO test method that:

> "The information provided by a rapid chloride permeability test (RCPT) or an AASHTO test is — at the most — equivalent to that which can be obtained by measuring the resistivity of the water-saturated sample.
>
> Neither RCPT, nor the resistivity measurement, can be taken as a measure of the diffusion resistance of the concrete, unless the conductivity of the porewater in that particular type of concrete and in that particular hydration state is known and the appropriate correction made.
>
> The results obtained in the RCPT cannot be used to calculate the diffusion coefficient (D) for chloride concrete and will therefore not allow predictions of chloride penetration with time."

Cao and Meck[22] state:

> "...the use of ASTM C 1202 as a tool for specifying materials would have a high probability of eliminating bad concrete mixes. However, it may preclude the most effective concrete mix.
>
> The problem appears to lie in the use of one classification table of ranking of chloride penetration for all materials. This would be the result of the binder dependent nature of the total charge passed."

We agree that correlations have been developed between the results of coulomb and ponding tests. Unfortunately, all of the correlations are different[23,24] and the correlations have wide scatter. This should preclude the use of the coulomb test as anything but the roughest of indicators.

5. ASTM T 259-Curing Period — We agree with Dr. Fidjestøl on the need for realistic curing periods in testing. Specimen ages used in the studies were those specified in AASHTO T 259; however, the 14-day curing period was modified to more realistically reflect the 7-day moist curing periods currently specified in ACI and AASHTO.

AASHTO 259 specifies an age of 42 days at the start of ponding. The normal storage of 28 days in a controlled climate room (CCR) at 72°F (23°C) with 50 percent relative humidity was extended to 35 days to account for the shortening of the 14-day curing period to 7 days. This period of air drying in a 50 percent relative humidity environment should be considered severe and representative of a longer drying period in a more moist environment. Note that the heat-cured specimen received only overnight heat curing, with no additional moist curing and all of the remaining time spent in the CCR.

6. Are De-icing Conditions Most Severe? — We disagree with Dr. Fidjestøl regarding his supposition that de-icing conditions are not the most severe; however, this may be the case in Scandinavian countries. In the United States, concrete deterioration of inland structures from de-icing salts has been of significantly more concern than coastal structures

from marine waters. He cites that rain waters may wash structures; however, this does not occur in covered structures.

7. Use of Diffusion Coefficients — The use of diffusion coefficients has received increased discussion from the research community. We agree, as stated in our paper, that limitations exist regarding the use of these techniques. As we stated, use of an "effective" coefficient on data from long-term ponding specimens is a useful tool for comparing chloride data sets and a great improvement over past methods such as comparing chloride contents at discrete locations or using "integral chloride" contents. Dr. Fidjestøl suggests that the chloride data in the paper is limited, even though we extended the AASHTO ponding period from 90 to 365 days. We do not believe that additional information would substantially change the conclusions of our paper.

8. Selection of Non-Optimal Concrete — Dr. Fidjestøl raises the question of selecting a "non-optimal" concrete mixture, without discussing what makes an "optimal" concrete. If impermeability alone is the controlling factor, then the 0.32 w/cm 7.5 percent silica fume concrete would be best, as stated in the conclusions of the paper. However, we will leave the question of "optimal" to the producers of the concrete to decide, taking into account the cost of materials, the cost of heat curing, permeability, strength, potential cracking problems, absorptions, and final appearance.

In his discussion, Dr. Hooton references a paper by Detwiler, Fapohunda and Natale titled "Use of Supplementary Cementing Materials to Increase the Resistance to Chloride Ion Penetration of Concretes Cured at Elevated Temperatures." Dr. Hooton incorrectly states that this study used proper preset times; however, in the discussion by McDonald and Pfeifer[25] and the subsequent reply by Detwiler et al., it is found that the concretes were cast using hot materials with no preset. Thus, the paper by Detwiler et al.[10] was not relevant to the present study.

We have recently reviewed the research by French and Mokhtarzadeh[9] where 7.5 percent silica fume was used as a replacement in moist-cured and heat-cured concretes with a total constant cementitious content of 445 kg/m^3 (750 lb/yd^3). These concretes were made with a rounded gravel and a crushed limestone. The heat-cured concrete utilized a 3-hour preset, followed by a 2.5-hour temperature rise to 150°F (71°C), held constant at 150°F (71°C) for 12 hours, and then a 2-hour temperature decrease period. The heat-cured concretes received no supplemental moist curing after the overnight heat curing. The data from this comprehensive study indicated the following:

- Very low w/cm ratio conventional and silica fume concretes do not suffer significant or meaningful 28-day strength losses when properly heat-cured, even with no supplemental moist curing.
- The heat-cured conventional concretes at 28 days with both aggregate types suffered essentially no strength loss when compared to the moist-cured conventional concrete, e.g., 97 to 99 percent of the moist strength, even with no supplemental moist curing.
- The heat-cured crushed limestone concretes with 7.5 percent silica fume replacement at 28 days suffered essentially no strength loss, e.g., 97 percent of the moist strength, while the heat-cured rounded gravel concrete with 7.5 percent silica fume replacement had significant strength loss, e.g., 86 percent of the moist-cured strength.
- The 7.5 percent silica fume content moist-cured concrete with limestone aggregate had only a 3 percent strength increase at 28 days due to fume, when compared to the conventional concrete. The same silica fume concrete that was heat-cured had only a 1 percent strength increase due to fume at 28 days.
- The 7.5 percent silica fume moist-cured concrete with rounded gravel had a 24 percent increase at 28 days when compared to the conventional concrete. The same silica fume concrete that was heat cured had a 8 percent strength increase at 28 days.

Table A. Times-to-corrosion for 0.46, 0.37 and 0.32 water-cementitious concretes.

Water-cementitious ratio	Control (heat)	5 percent silica fume	7.5 percent silica fume
0.46	4	12	13
0.37	11	25	25
0.32	20	28	38

Dr. Hooton's discussion of Table 1 in the current study regards factors to be kept constant in mixture designs for research programs. In this study, the water contents for the control mixtures were kept constant for the three water-cementitious (w/cm) ratios. For the mixtures containing silica fume, the silica fume was used as an addition to the cementitious content. Water was added to the silica fume mixtures to keep constant w/cm ratios. The methods chosen by the authors were based on the usual specification requirements that state a maximum w/cm ratio.

Silica fume is also frequently used as an addition to the cement, rather than as a replacement. If the guidance of Dr. Hooton is correct, then manufacturers of silica fume need to make users aware that the permeability of concrete containing silica fume is extremely sensitive to total cementitious and water content, and less sensitive to w/c or w/cm ratio.

We agree that lower water-cement ratios are possible through the use of high range water reducers; however, such additions would limit the ability of the data to be rationally analyzed. Because of the permeability improvements given to concrete by the use of a high range water reducing agent (HRWRA),[23] the dosages of the HRWRA were held relatively close for the different w/cm concretes to minimize the effect of the HRWRA on the results. If the HRWRA dosage had been increased for the silica fume mixtures, the effect of the HRWRA could not have been differentiated from the effect of the silica fume.

As discussed above, the AASHTO T 259 test was used extensively, as this is required by ASTM C 1202. We agree with Dr. Hooton that modifications to the T 259 tests are required to improve the quality of data from this test. Possibly, ASTM could develop a better test than the AASHTO T 259 test that is currently specified in ASTM C 1202.

Diffusion profiles obtained from AASHTO T 259 include absorption obtained from the initial wetting of the slabs with

the chloride solution, and chemically-bound chloride in the concrete. As such, the reported diffusion coefficients are based on smeared diffusion/absorption values. Real concretes are also subject to drying and will have absorption, and this absorption may dominate the first 10 to 20 mm (0.4 to 0.8 in.) of the concrete. The issue of absorbed and diffused chloride ions needs additional research, and tests for these elements require standardization. We still believe that the effective diffusion coefficients and surface concentrations determined from our data provide useful and realistic information for ranking material performance.

Dr. Hooton does not believe Conclusion 9 of our paper, which states that the times-to-corrosion of the 0.37 w/cm silica fume concretes are similar to those of the heat-cured 0.37 to 0.32 w/cm plain concretes. This statement was misquoted by Dr. Hooton. Conclusion 9 states that the times-to-corrosion of the 0.46 and 0.37 w/cm silica fume concretes are similar to those of the heat-cured 0.37 to 0.32 w/cm plain concretes. The data are shown in Table A.

We still consider that the 0.37 and 0.46 w/cm concretes with 5 or 7.5 percent silica fume and calculated times-to-corrosion of 12 and 13, 25 and 25 years are similar to that of the 0.32 and 0.37 w/c heat-cured concretes and calculated their times-to-corrosion of 11 and 20 years.

The authors agree that if coulomb and diffusion data are plotted on logarithmic scales, an apparent relationship is found. The issue is not whether one can fit a straight line to the data, but whether one is able to use the information in specifications to limit concrete to a particular coulomb value, such as 1000. Fig. F from Dr. Hooton shows one concrete with a diffusion value of 0.6×10^{12} m^2/s and a coulomb value of 750 and another concrete with a diffusion value of 0.3×10^{12} m^2/s and a coulomb value of 2000. Thus, higher coulomb readings are not always indicative of higher diffusion, nor are lower coulomb readings indicative of lower diffusion. There is no doubt that the use of a rigidly specified coulomb value of say 1000 is wrong.

If Dr. Hooton believes the final recommendation that the ASTM C 1202 rapid chloride test can be used with confidence to predict chloride diffusion rate, and that he would certainly not recommend correlating it with the T 259 chloride ponding test, then we suggest that he act, along with the authors, to remove such recommendations from the ASTM C 1202 test procedure.

REFERENCES

9. French, C. W., and Mokhtarzadeh, A., "High Strength Concrete: Effects of Materials, Curing and Test Procedures on Short-Term Compressive Strength," PCI JOURNAL, V. 38, No. 3, May-June 1993, pp. 76-87.
10. Detwiler, R. J., Kjellsen, K. O., and Gjorv, O. E., "Resistance to Chloride Intrusion of Concrete Cured at Different Temperatures," *ACI Materials Journal*, V. 88, No. 1, January-February 1991, pp. 18-24.
11. Perenchio, W. F., Disc. "Resistance to Chloride Intrusion of Concrete Cured at Different Temperatures" by Detwiler, Kjellsen, and Gjorv, *ACI Materials Journal*, V. 88, No. 6, November-December 1991, pp. 676-679.
12. McDonald, D. B., Disc. "Durability of Concrete Incorporating High Volumes of Fly Ash From Sources in the U.S.," *ACI Materials Journal*, V. 91, No. 6, November-December 1994, pp. 632-633.
13. McDonald, D. B., and Pfeifer, D. W., Disc. "Use of Supplementary Cementing Materials to Increase the Resistance to Chloride Ion Penetration of Concretes Cured at Elevated Temperatures," by Detwiler, Fapohunda, and Natale, *ACI Materials Journal*, V. 91, No. 6, November-December 1994, pp. 636-638.
14. McDonald, D. B., and Sherman, M. R., Disc. "Properties of Silica Fume Concrete and Mortar," by Bayasi and Zhou, *ACI Materials Journal*, V. 91, No. 3, May-June 1994, p. 320.
15. Torrii, K., and Kawamura M., "Pore Structure and Chloride Ion Permeability of Mortars Containing Silica Fume," *Cement and Concrete Composites*, V. 16, 1994, pp. 279-286.
16. Zhang, T., and Gjorv, O. E., "An Electrochemical Method for Accelerated Testing of Chloride Diffusivity in Concrete," *Cement and Concrete Research*, V. 8, 1994, pp. 1534-1548.
17. Berke, N. S., Dallaire, M. P., and Hicks, M. C., "Plastic, Mechanical, Corrosion, and Chemical Resistance Properties of Silica Fume (Microsilica) Concretes," Proceedings, Fourth International Conference on Fly Ash, Silica Fume, Slab, and Natural Pozzolans in Concrete, Special Publication SP-132, American Concrete Institute, Farmington Hills, MI, 1992, pp. 1125-1149.
18. Berke, N. S., Scali, M. J., Regan, J. C., and Shen, D. F., "Long-Term Corrosion Resistance of Steel in Silica Frame and/or Fly Ash Containing Concretes," Proceedings, Second International Conference on Durability of Concrete, Special Publication SP-126, American Concrete Institute, Farmington Hills, MI, 1991, pp. 393-421.
19. Whiting, D., and Mitchell, T. M., "A History of the Rapid Chloride Permeability Test," Transportation Research Record 1335, Washington, D. C., 1992.
20. Andrade, C., "Calculation of Chloride Diffusion Coefficients in Concrete From Ionic Migration Measurements," *Cement and Concrete Research*, V. 23, 1993, pp. 724-742.
21. Arup, H., Sorenseon, B., Frederiksen, J., and Thaulow, N., "The Rapid Chloride Permeability Test — An Assessment," Presented at NACE Conference-93, New Orleans, LA, March 7-12, 1993.
22. Cao, H. T., and Meck, E., "A Review of the ASTM C 1202 Standard Test," *Concrete in Australia*, October 1996.
23. Pfeifer, D. W., McDonald, D. B., and Krauss, P. D., "The Rapid Chloride Permeability Test and Its Correlation to the 90-Day Chloride Ponding Test," PCI JOURNAL, V. 39, No. 1, January-February 1994, pp. 38-47.
24. Scanlon, J. M., and Sherman, M. R., "Fly Ash Concrete: An Evaluation of Chloride Penetration Testing Methods," *Concrete International*, V. 18, No. 6, June 1996, pp. 57-62.
25. McDonald, D. B., and Pfeifer, D. W., Disc. "Use of Supplementary Cementing Materials to Increase the Resistance to Chloride Ion Penetration of Concretes Cured at Elevated Temperatures," by Detwiler, Fapohunda, and Natale, *ACI Materials Journal*, V. 91, No. 6, November-December 1994, pp. 636-638.

Shear Behavior of Full-Scale Prestressed Concrete Girders: Comparison Between AASHTO Specifications and LRFD Code*

by Mohsen A. Shahawy and Barrington deV Batchelor

Comments by Kris G. Bassi, Michael P. Collins, John M. Kulicki, Scott R. Eshenaur, and Andrew L. Thomas, and Authors' Closure

KRIS G. BASSI†

The last sentence in the first paragraph in the left column on page 49 of the paper states that "It should be noted that like the AASHTO Specifications (1977), the OHBDC (1993) also provides for the use of the 45-degree truss analogy in a simplified shear design method." This statement is not correct as far as OHBDC is concerned. The draft of the forthcoming Canadian Highway Bridge Design Code (CHBDC) allows a simplified method based on a 45-degree truss analogy only for non-prestressed components that are not subject to axial tension.

MICHAEL P. COLLINS‡

The authors have conducted an impressively extensive experimental investigation that is aimed at providing some answers to the question "Are the 1994 AASHTO LRFD shear design provisions any better than the 1989 AASHTO and 1995 ACI shear design provisions?" While the experimental results are of considerable value, the analyses of these results given in the paper are seriously flawed and lead the authors to make inappropriate conclusions. Further, the writer disagrees with the authors' contention that adoption of the new provisions "requires engineers to expend more effort on shear design."

COMPARISONS OF 1994 LRFD AASHTO AND 1989 AASHTO DESIGNS

The authors determined the stirrup layout for the "basic girder" of the test series by designing this member using the 1989 AASHTO Specifications for a 40 ft (12.2 m) span simply supported bridge with girders spaced at 10 ft (3.05 m). It makes an interesting comparison to redesign this girder using the shear design provisions of the 1994 AASHTO LRFD Specifications. To make the comparison more direct, only the shear design procedures will be changed, while the loads and load factors of the 1989 Specifications will be retained.

Fig. A gives the maximum factored moments that occur at the tenth points of the span due to dead load [assumed to be 2 kips per ft (29.2 kN/m)] and live load and impact associ-

* PCI JOURNAL, V. 41, No. 3, May-June 1996, pp. 48-62.
† Consulting Engineer, Etobicoke, Ontario, Canada.
‡ Professor, Department of Civil Engineering, University of Toronto, Toronto, Ontario, Canada.

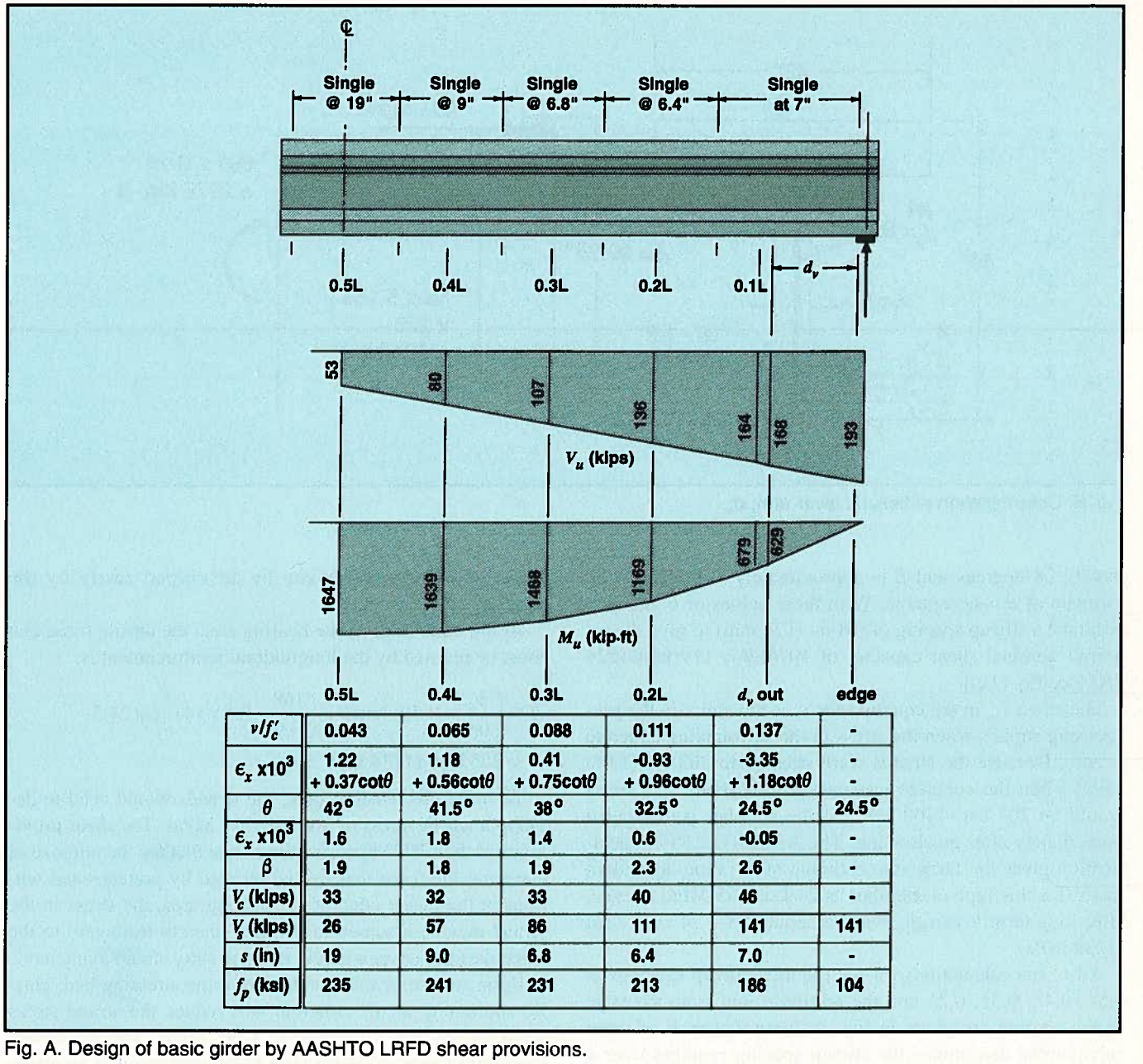

v/f_c'	0.043	0.065	0.088	0.111	0.137	-
ϵ_x x10^3	1.22 + 0.37cotθ	1.18 + 0.56cotθ	0.41 + 0.75cotθ	-0.93 + 0.96cotθ	-3.35 + 1.18cotθ	- -
θ	42°	41.5°	38°	32.5°	24.5°	24.5°
ϵ_x x10^3	1.6	1.8	1.4	0.6	-0.05	-
β	1.9	1.8	1.9	2.3	2.6	-
V_c (kips)	33	32	33	40	46	-
V_s (kips)	26	57	86	111	141	141
s (in)	19	9.0	6.8	6.4	7.0	-
f_p (ksi)	235	241	231	213	186	104

Fig. A. Design of basic girder by AASHTO LRFD shear provisions.

ated with the passage of an HS20 truck. The cross section of the girder is described in Fig. B, which also illustrates that the flexural capacity of this section will be about 2076 kip-ft (2815 kN-m) and that the effective shear depth will be 37.7 in. (957 mm).

By the AASHTO LRFD method, the nominal shear capacity, V_n, is given by:

$$V_n = 0.0316\beta\sqrt{f_c'}b_v d_v + \frac{A_v f_y}{s} d_v \cot\theta$$
$$= 0.0316\beta\sqrt{6}\times 6\times 37.7 + \frac{0.2\times 60\times 37.7}{s}\cot\theta$$
$$= 17.5\beta + \frac{452}{s}\cot\theta \text{ kips} \qquad (12)$$

The values of β and θ are given in tables and charts in the LRFD Specifications. The chart for members with web reinforcement is given here as Fig. C. In this chart, β and θ are functions of the shear stress ratio v/f_c' and the longitudinal strain ϵ_x, where:

$$\frac{v}{f_c'} = \frac{V_u}{\phi b_v d_v f_c'} = \frac{V_u}{0.9\times 6\times 37.7\times 6} = \frac{V_u}{1221}$$

Thus, at 0.3L, the shear stress ratio is 107/1221 = 0.088. The strain ϵ_x at 0.3L is:

$$\epsilon_x = \frac{M_u/d_v + 0.5V_u\cot\theta - A_{ps}f_{po}}{E_p A_{ps}}$$
$$= \frac{1468/3.14 + 0.5\times 107\cot\theta - 2.448\times 179}{29000\times 2.448} \qquad (13)$$
$$= 0.41\times 10^{-3} + 0.75\times 10^{-3}\cot\theta$$

With an estimate of 38 degrees for θ, this will give a value of 1.38 × 10^{-3} for ϵ_x. For v/f_c' = 0.088 and ϵ_x equal to 1.38 × 10^{-3}, it can be seen from the chart that θ is approxi-

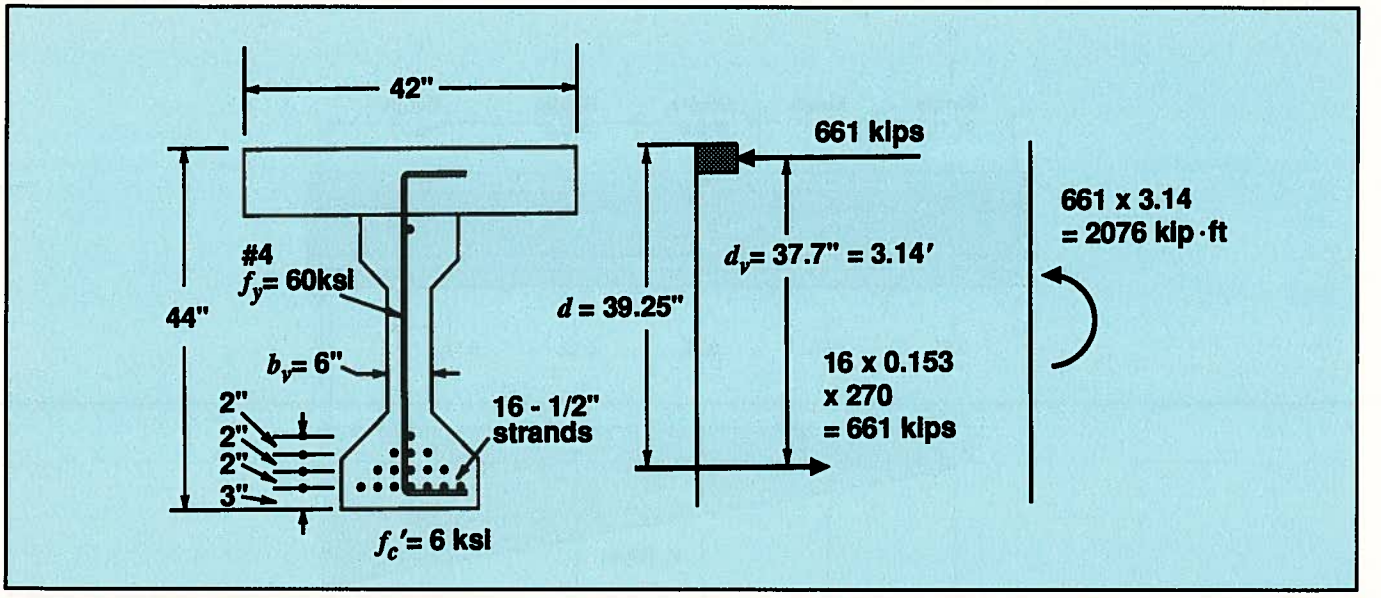

Fig. B. Determination of flexural lever arm, d_v.

mately 38 degrees and β is approximately 1.9. Hence, the estimate of θ is acceptable. With these values of θ and β, it will take a stirrup spacing of 6.8 in. (173 mm) to give the required nominal shear capacity of 107/0.9 = 119 kips (529 kN) [see Eq. (12)].

The stress f_{po} in the equation for ε_x is the stress in the prestressing strands when the stress in the surrounding concrete is zero. Because the strands were stressed to 203 ksi (1400 MPa) when the concrete was cast around them, this stress would be 203 ksi (1400 MPa) if the member were loaded immediately after prestressing. The AASHTO-LRFD Specification gives the lump sum estimate of the time-dependent losses for this type of member as 24 ksi (165 MPa). Hence, after long-term losses, f_{po} will be about 203 – 24 = 179 ksi (1234 MPa).

All of the calculations for the required stirrup spacings at 0.5L, 0.4L, 0.3L, 0.2L and the section d_v out from the edge of the bearing are given in Fig. A. Note that each of these calculations determines the stirrup spacing required over a certain length of the beam, with the calculated section being in the middle of this length (see Fig. A).

It is the writer's experience that determining the required stirrup spacings along the length of a bridge girder by the 1989 AASHTO Specifications or the 1995 ACI method takes more work than doing the same task with the 1994 AASHTO LRFD procedure. With the ACI procedure, the calculation of the flexure-shear cracking load, V_{ci}, requires consideration of individual load combinations and the calculation of the concrete stress history of the composite sections.

A key feature of the new LRFD shear provisions is that they explicitly consider the influence of shear on the longitudinal reinforcement. The required stress in the longitudinal strands of the bridge girder is:

$$f_{ps} = \left[\frac{M_u}{3.14} + \left(\frac{V_u}{0.9} - 0.5V_s\right)\cot\theta\right] / 2.448$$

The values given by this expression for the sections at 0.5L, 0.4L, 0.3L, 0.2L and d_v out are listed in Fig. A. All of these required stresses can be developed easily by the strands.

At the inner edge of the bearing area, the tensile force that must be resisted by the longitudinal reinforcement is:

$$T = \left(\frac{V_u}{0.9} - 0.5V_s\right)\cot\theta = \left(\frac{168}{0.9} - 0.5\times 141\right)\cot 24.5$$

$$= 255 \text{ kips (1134 kN)}$$

To resist this tension force, the strands would need to develop a tensile stress of 104 ksi (717 MPa). The shear provisions of the LRFD Specifications state that for the purpose of checking the force that can be resisted by pretensioned tendons at the inside edge of the bearing area, the stress in the strand may be assumed to increase linearly from zero to the effective stress over a length equal to sixty strand diameters.

Upon release of the member from the stressing bed, elastic shortening of the concrete will reduce the strand stress from 203 to 188 ksi (1400 to 1296 MPa). The additional long-term losses of 24 ksi (165 MPa) will result in an effective stress of 164 ksi (1130 MPa). As the inner edge of the bearing is only about 10 in. (254 mm) from the free end of the strand, the tension in the strands at this location can be taken as:

$$T_{strands} = \frac{10}{60\times 0.5}\times 164\times 2.448 = 134 \text{ kips (596 kN)}$$

Because 134 kips (596 kN) is less than 255 kips (1134 kN), additional longitudinal reinforcement is required at this location.

Area of Grade 60 longitudinal reinforcement required

$$= \frac{255-134}{60} = 1.90 \text{ sq in. (1226 mm}^2\text{)}$$

Use four #5 U-bars 34 in. (863 mm) long.

Area = 4 × 2 × 0.31 = 2.48 sq in. (1600 mm^2)

The reinforcement pattern determined from the 1994 AASHTO LRFD shear design procedures, Design B, is compared with the pattern obtained from the 1989

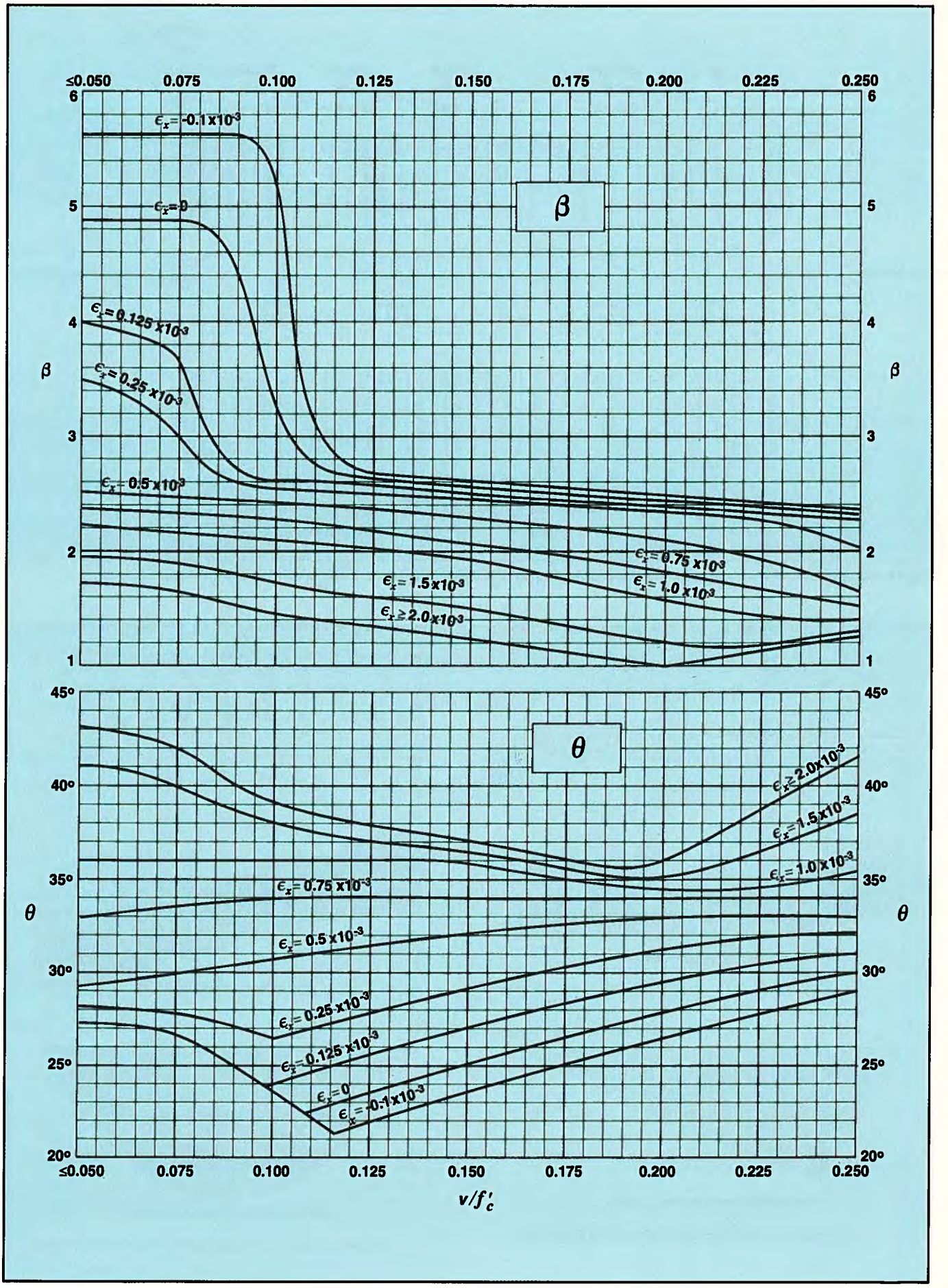

Fig. C. Values of θ and β for sections with transverse reinforcement.

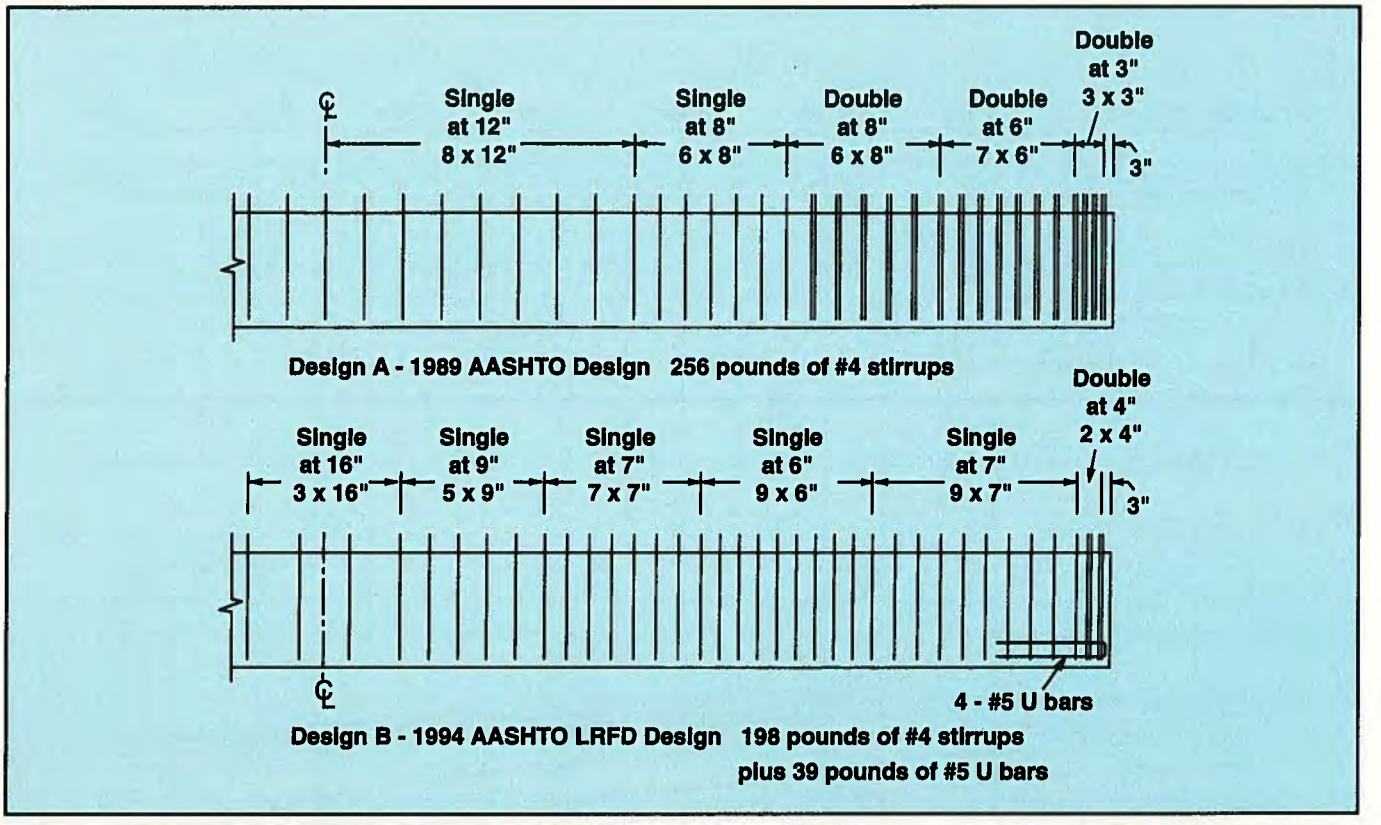

Fig. D. Comparison of reinforcement patterns obtained by 1989 AASHTO and 1994 AASHTO LRFD shear designs.

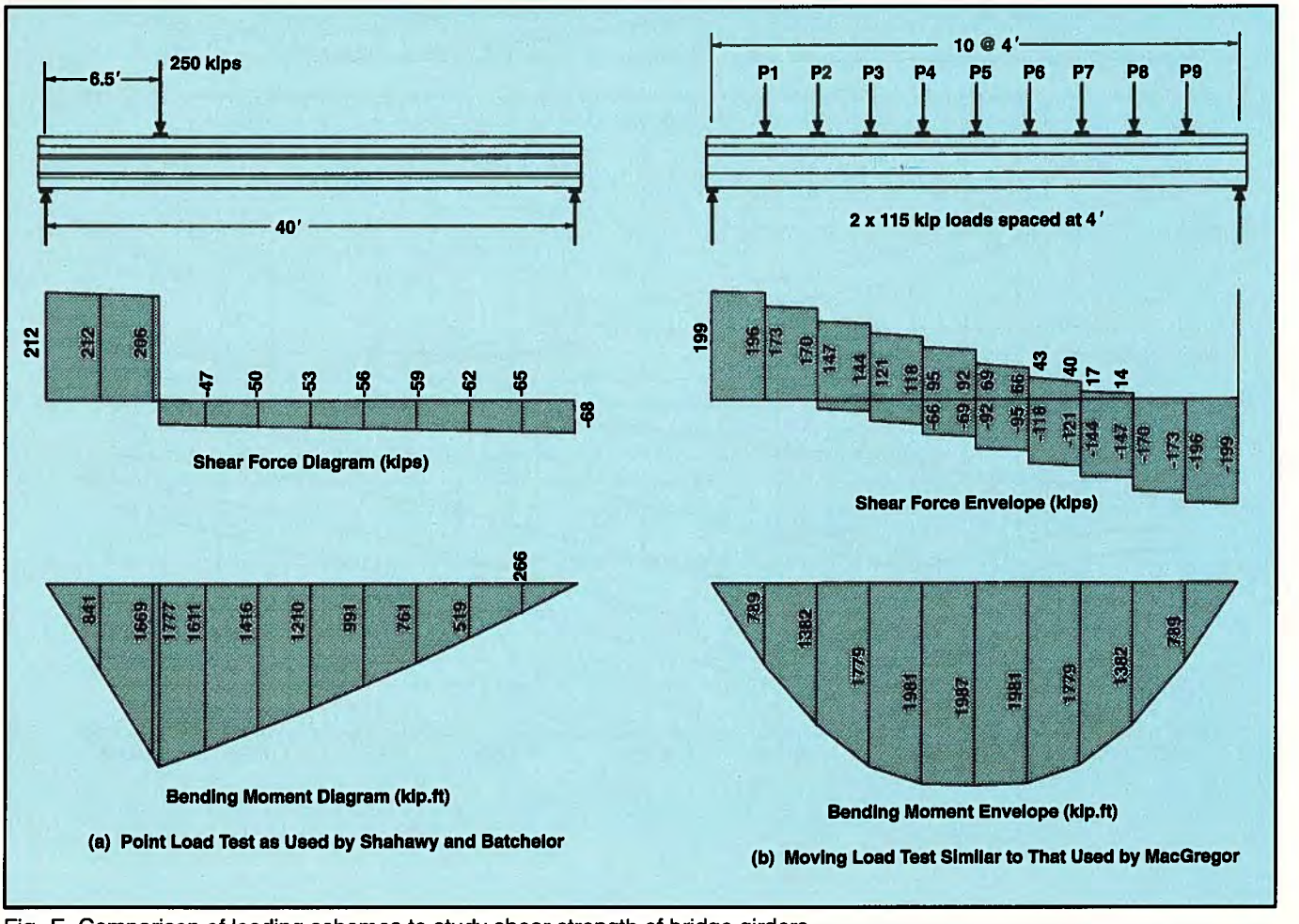

Fig. E. Comparison of loading schemes to study shear strength of bridge girders.

AASHTO procedure, Design A, in Fig. D. While the two designs use about the same amount of reinforcement (the reinforcing bar weight is 7 percent less in Design B), the distribution of the reinforcement is substantially different. In the middle 24 ft (7.3 m) of the girder, Design A has 20 percent fewer stirrups than Design B. In the outer 17 ft (5.2 m) of the girder [8 ft 6 in. (2.6 m) each end], Design A has 78 percent more stirrups than Design B, but Design B contains the additional longitudinal U-bars over the bearing area, which are intended to prevent bond failures in this region.

It would make an excellent comparison of the merits of the two different shear design procedures if two girders representing Design A and Design B were loaded to failure under simulated truck loading.

COMMENTS ON LOADING SCHEME USED IN INVESTIGATION

The authors arranged the pattern of stirrups in their girders to resist the shears and moments associated with the passage of an AASHTO HS20 truck. They then tested the girders by applying a point load quite close to a support and increasing this load until failure occurred. Unfortunately, the pattern of shears and moments produced by this type of loading differs substantially from that caused by a moving load. Compare Figs. E and A.

A more realistic loading would have been obtained if, say, nine jacks had been installed along the length of the beam and then pairs of jacks had been loaded sequentially. Thus, for the scheme shown in Fig. E, Jacks P_1 and P_2 would first be loaded, then P_2 and P_3, then P_3 and P_4, and so on. This loading would simulate the effects of a pair of wheel loads, spaced 4 ft (1.2 m) apart, passing over the girder. Such a loading scheme would have provided a much more comprehensive test of the shear performance of the girders. This type of simulated moving load was used nearly 40 years ago by James G. MacGregor[9] in his doctoral research on the shear resistance of prestressed concrete bridge girders.

The point load test used by the authors has the advantage that it is easy to conduct. MacGregor reports that a fixed point load test similar to that used by Shahawy and Batchelor took about 4 hours to complete while a simulated moving load test took 2 days to complete. However, if a point load test is to be used, the shear reinforcement should be designed for this pattern of loads. Further, the point load experiments of the authors' test only the end regions of the girders.

PREDICTED STRENGTHS OF TEST BEAMS BY AASHTO LRFD PROCEDURE

The shear design procedures of the AASHTO LRFD Specifications were formulated to be convenient for design. They are less convenient for use in predicting the shear strength of a given member under a given loading. Further, the authors have demonstrated that, in this case, the procedures can be misinterpreted to produce unsatisfactory results. The writer would like to clarify a number of points about this application of the new procedures.

In predicting the strengths of the beams tested by the authors, it is necessary to check the three modes of failure illustrated in Fig. F. Mode 1 involves yielding of the longitudinal reinforcement at the maximum moment location, which results in a flexural failure under the point load. Mode 2 involves yielding of the stirrups over a substantial length of the beam, which results in a shear-flexure failure in the region adjacent to the point load. Mode 3 involves slipping of the strands over the bearing, which results in a shear-bond failure in the region adjacent to the support. Modes 2 and 3 involve inclined failure surfaces, which in the calculations are approximated by the vertical Sections LL and SS at mid-length of the inclined failure surfaces. While it would be more accurate to take the distance from the face of the support to Section SS and the distance from the face of the load to Section LL as $0.5d_v\cot\theta$, the AASHTO LRFD Specifications allow us to approximate these distances as d_v.

As an example of the calculations, let us consider the test of the south end of Specimen A1-00-R. This girder had a concrete strength of about 7.11 ksi (49 MPa) and the stirrups in the girder had a yield strength of about 70 ksi (482 MPa).

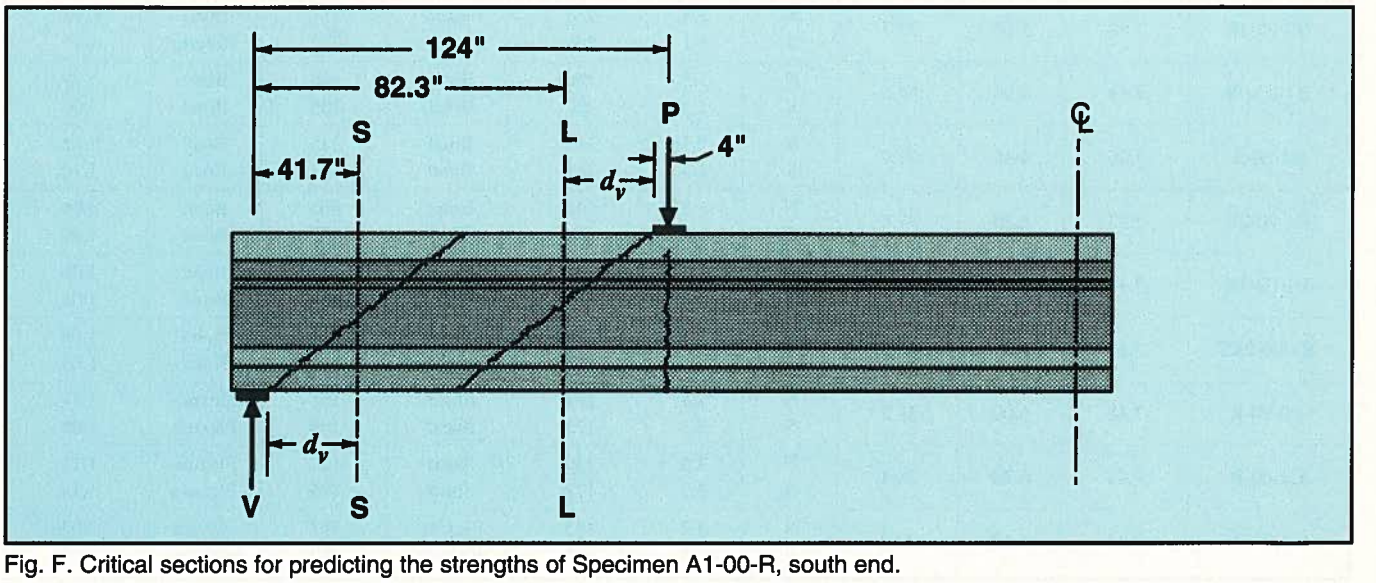

Fig. F. Critical sections for predicting the strengths of Specimen A1-00-R, south end.

The shear that would cause flexural failure is:

$$V_{flex} = \frac{2076 \times 12}{124} = 201 \text{ kips (894 kN)}$$

At Section LL, the shear strength is:

$$V = 0.0316\beta\sqrt{f_c'}b_v d_v + \frac{A_v f_y}{s} d_v \cot\theta$$
$$= 0.0316\beta\sqrt{7.11} \times 6 \times 37.7 + 0.0428 \times 70 \times 37.7 \cot\theta$$
$$= 19.1\beta + 113\cot\theta \quad (14)$$

where the stirrup amount A_v/s has been taken as the average amount in a length of $2d_v$ centered on Section LL.

The most convenient procedure for determining β and θ is to assume a value for the failure shear, determine v/f_c' and ε_x, find β and θ from Fig. C and then check the assumed value of shear from Eq. (14). Thus, if we estimate that $V = 185$ kips (823 kN):

$$\frac{v}{f_c'} = \frac{V}{7.11 \times 6 \times 37.7} = \frac{V}{1608} = \frac{185}{1608} = 0.115$$

From Eq. (13):

$$\varepsilon_x = \frac{185 \times 82.3/37.7 + 0.5 \times 185\cot\theta - 2.448 \times 179}{29000 \times 2.448}$$
$$= -0.48 \times 10^{-3} + 1.30\cot\theta$$

Table A. Comparison of observed and predicted shear strengths.

Specimen	f_c' (ksi) Beam	f_c' (ksi) Slab	d_v (in.)	End	a/d	Predicted V (kips)	Predicted Mode	Test V (kips)	Test Mode	Test / Predicted
A0-00-R	8.48	5.50	37.6	N	2.1	208	Bond	313	Bond	1.50
				S	2.1	208	Bond	276	Shear	1.33
A1-00-M	7.30	5.50	37.6	N	2.5	119	Bond	141	Bond	1.18
				S	3.1	119	Bond	168	Bond	1.41
A1-00-R/2	7.10	5.50	37.6	N	2.5	153	Bond	166	Bond	1.09
				S	3.1	153	Bond	173	Bond	1.13
A1-00-R	7.11	5.93	37.7	N	2.5	207	Bond	210	Bond	1.01
				S	3.1	185	Shear	208	Flexure	1.12
A1-00-3R/2	7.60	6.70	37.9	N	2.5	246	Flexure	207	Bond	0.84
				S	3.1	202	Flexure	230	Flexure	1.14
A2-00-2R	7.03	5.33	37.5	N	2.5	244	Flexure	257	Flexure	1.05
				S	1.8	252	Bond	357	Flexure	1.42
A2-00-3R	7.30	5.10	37.4	N	2.5	243	Flexure	257	Flexure	1.06
				S	2.1	252	Bond	312	Flexure	1.24
A4-00-0R1	7.60	5.50	37.6	N	2.3	89	Bond	94	Shear	1.06
				S	2.3	89	Bond	98	Shear	1.10
A4-00-0R2	7.45	5.10	37.4	N	1.8	89	Bond	101	Shear	1.13
				S	1.8	89	Bond	106	Shear	1.19
B0-00-R	7.45	4.09	37.2	N	2.5	207	Bond	220	Bond	1.06
				S	3.1	186	Shear	206	Shear	1.11
B0-00-2R	7.23	4.03	37.2	N	2.5	247	Flexure	223	Bond	0.90
				S	3.1	203	Flexure	216	Flexure	1.06
B0-00-3R	7.68	5.10	37.7	N	2.5	250	Flexure	231	Bond	0.92
				S	3.1	206	Flexure	236	Flexure	1.15
B1-00-0R	7.19	4.90	37.6	N	1.5	88	Bond	166	Bond	1.89
				S	1.3	88	Bond	155	Bond	1.76
B1-00-R	7.46	4.46	37.4	N	1.5	211	Bond	245	Bond	1.16
				S	1.3	211	Bond	232	Bond	1.10
B1-00-2R	7.82	5.20	37.7	N	1.5	248	Bond	262	Bond	1.06
				S	1.3	248	Bond	247	Bond	1.00
B1-00-3R	7.45	5.30	37.7	N	1.5	248	Bond	264	Bond	1.06
				S	1.3	248	Bond	263	Bond	1.06
B1-00-2R2	7.28	4.83	37.6	N	1.5	248	Bond	268	Bond	1.08
				S	1.3	248	Bond	255	Bond	1.03
C0-00-R	7.48	6.00	38.2	N	3.5	159	Shear	176	Flexure	1.11
				S	3.2	172	Shear	180	Flexure	1.05
C1-00-R	7.42	6.70	38.4	N	3.5	159	Shear	177	Flexure	1.11
				S	3.2	172	Shear	196	Flexure	1.14
C1-00-3R/2	7.23	6.10	38.3	N	3.2	185	Flexure	192	Flexure	1.04
				S	3.1	194	Flexure	202	Flexure	1.04

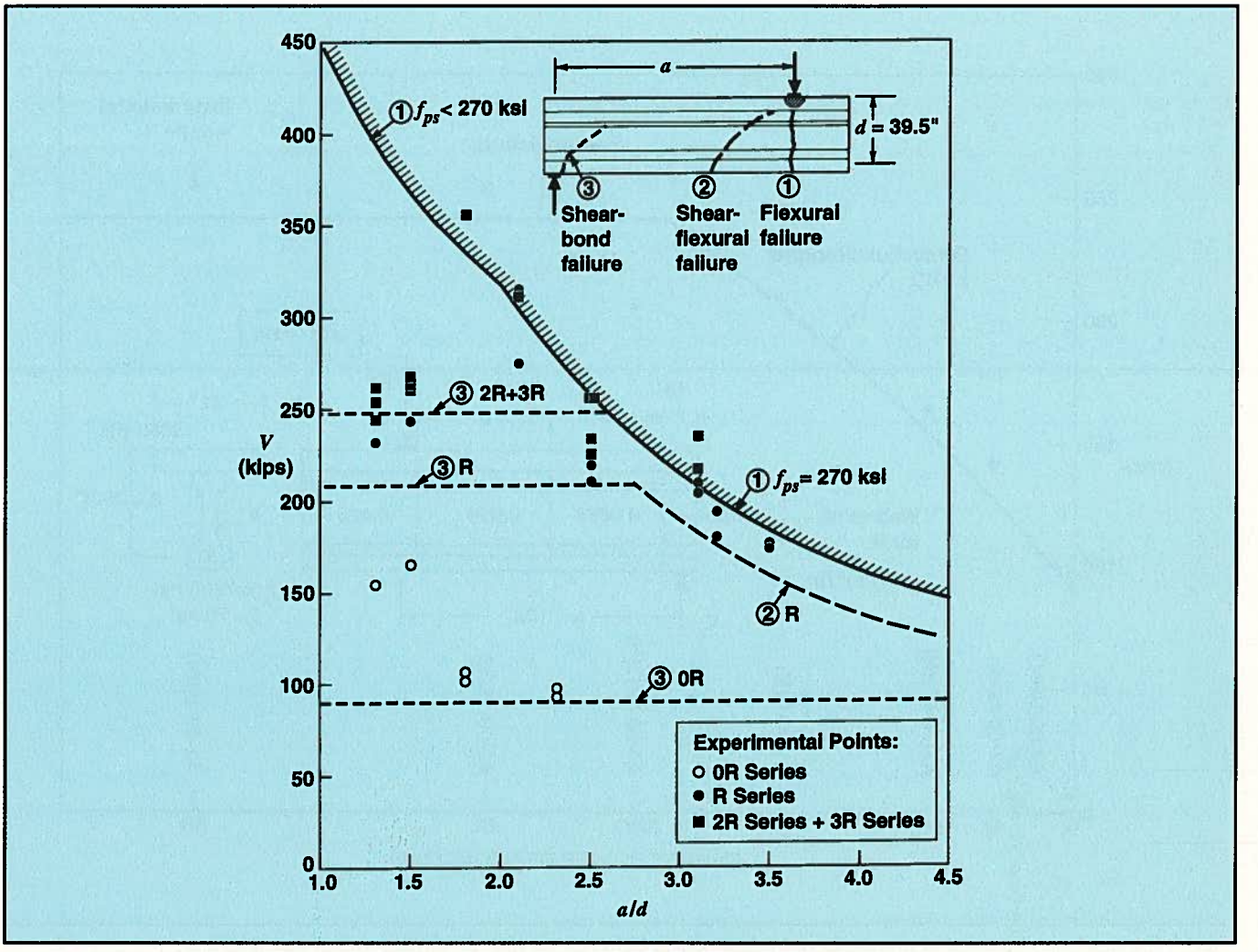

Fig. G. Comparison of predicted and observed failure shears for 0R, R, 2R and 3R series.

With θ taken at 36.5 degrees, the value of ε_x from Eq. (13) is 1.28×10^{-3}. For this value of ε_x and with $v/f_c' = 0.115$, the chart in Fig. C gives $\theta = 36.7$ degrees and $\beta = 1.8$. These values result in a shear of:

$$V = 19.1 \times 1.8 + 113 \cot 36.7$$
$$= 34.4 + 151.6 = 186 \text{ kips (827 kN)}$$

Thus, our estimate of 185 kips (823 kN) for the shear strength at Section LL is accurate.

At Section SS, the shear strength is:

$$V = 19.1\beta + 0.0615 \times 70 \times 37.7 \cot\theta$$
$$= 19.1\beta + 162 \cot\theta \quad (15)$$

Because there are more stirrups at Section SS than at Section LL and the moment at SS is lower than at LL, our concern is not with a shear-flexure failure but rather with a shear-bond failure involving slip of the tendons. The AASHTO LRFD requires that the tendons resist a tension at the inner edge of the bearing area of:

$$T = \left(\frac{V_u}{\phi} - 0.5V_s\right)\cot\theta \quad (16)$$

This relationship was derived by Collins and Mitchell[5] as:

$$T = V_c \cot\theta + 0.5V_s \cot\theta \quad (17)$$

and then was reformulated as Eq. (16) using the assumption that:

$$\frac{V_u}{\phi} = V_c + V_s \quad (18)$$

Note that to satisfy the basic relationship of Eq. (17), which tells us that shear carried by stirrups causes just half as much tension in the longitudinal reinforcement as shear carried by concrete mechanisms, the value of V_s in Eq. (16) should not be taken as greater than V_u/ϕ. That is, the tension should not be less than $0.5(V_u/\phi)\cot\theta$.

For Specimen A1-00-R, the strands can resist a tension of 134 kips (596 kN) at the inner edge of the bearing. Hence:

$$134 \geq (V - 0.5 \times 162 \cot\theta)\cot\theta \quad (19)$$

but

$$134 \geq 0.5V\cot\theta \quad (20)$$

The values of θ and the corresponding β values given in Fig. C were chosen to minimize the amount of stirrup reinforcement. If excess stirrups have been provided, then the θ and β values associated with larger values of ε_x can be used to reduce the demand on the longitudinal reinforcement. The lowest tension will be associated with the highest values of θ and the corresponding β values. The highest value of θ is

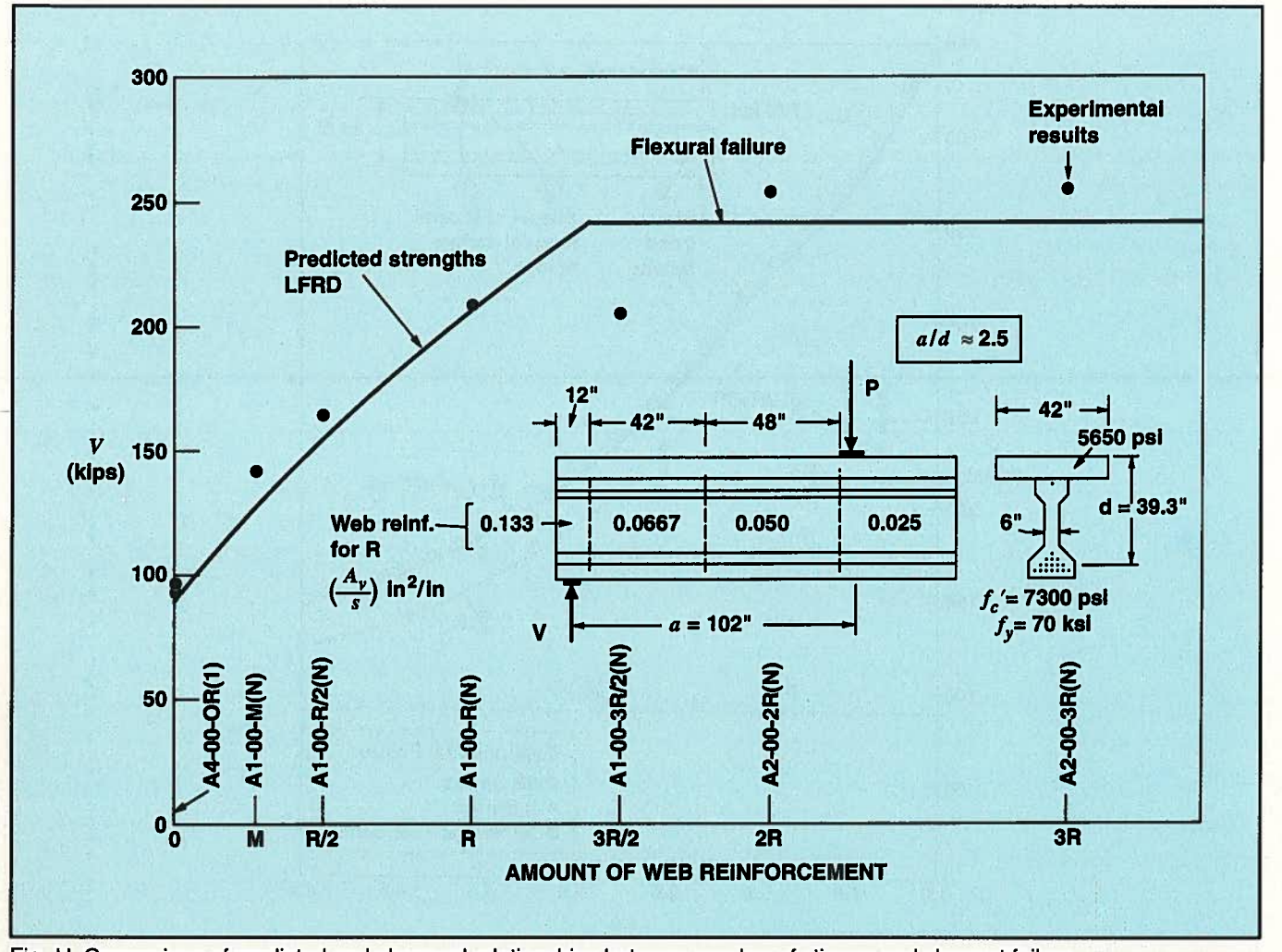

Fig. H. Comparison of predicted and observed relationships between number of stirrups and shear at failure.

43 degrees, with a corresponding β value of 1.72. With these values, Eq. (15) gives a shear failure value of 207 kips (921 kN), Eq. (19) gives 212 kips (943 kN) and Eq. (20) gives 250 kips (1112 kN). Hence, the estimate for the failure shear at the support is 207 kips (921 kN).

Thus, we predict that the south end of Specimen A1-00-R will fail in shear-flexure, near the point load, at a shear of 185 kips (823 kN). The authors report that this test failed in flexure at a shear of 208 kips (925 kN). Their detailed test report[7] shows that this member had wide diagonal cracks near the point load.

The above calculations were repeated for the 40 tests reported by the authors and the resulting predictions are shown in Table A. Note that 24 of the 40 tests are predicted to have their strength governed by slipping of the strands over the bearing. In view of the usual variability of bond strength, it is perhaps surprising that the results are so consistent. In the writer's opinion, one of the major contributions of the authors' extensive experimental study is to show that bond-slip failures of pretensioned prestressing strand are relatively ductile and reasonably predictable.

Fig. G summarizes the predicted and observed shear strengths for the 32 tests that made up the 0R, R, 2R and 3R series. The figure shows how the failure shear changes as the shear span is changed and the amount of shear reinforcement is changed. It is interesting that the 2R and 3R series are predicted to have the same strengths and that the shear span-to-depth ratio is predicted not to influence the failure shear of members failing in Mode 3 (i.e., strand slip failures).

Note that only the R series of beams with a/d values greater than about 2.7 are predicted to fail in Mode 2 (i.e., shear-flexure failures). In considering the two members with no stirrups (0R series) with low a/d ratios that failed at such relatively high shears, it is important to know that these "beams" failed upon the formation of the first diagonal crack. The new LRFD shear provisions are concerned with predicting post-cracking shear capacity rather than predicting first cracking load.

The manner in which the strength of the members, tested with a shear span-to-depth ratio of 2.5, increased as the amount of stirrups increased is illustrated in Fig. H. In the end regions of the beams, the amount of shear reinforcement used for the standard R series was rather large, resulting in a value of $A_v f_y/(b_v s)$ of 778 psi (5.4 MPa), which is about 15 times the traditional minimum web reinforcement of 50 psi (0.34 MPa). As a result of this large amount, very little increase in capacity was predicted when the amount of shear reinforcement was made even larger. It can be seen from Fig. H that the predictions based on the new AASHTO LRFD shear provisions agree well with the observed test results.

CONCLUDING REMARKS

It is the writer's opinion that one of the chief advantages of the new AASHTO LRFD shear design provisions is that they direct the engineer's attention to the possibility of a shear-bond failure at the end of the beam. The efficient way to suppress such failures is to provide additional well-anchored reinforcing bars over the support.

In addition to being general and rational, the new shear design provisions result in somewhat simpler designs for prestressed girders and lead to more accurate predictions of shear capacity. In a study of 528 test results,[10] which included most of the authors' tests, the mean ratio of experimental to predicted failure load was 1.32 with a coefficient of variation of 33.7 percent for the ACI shear design provisions, and 1.39 with a coefficient of variation of 19.7 percent for the AASHTO LRFD provisions.

REFERENCES

9. MacGregor, J. G., "Strength and Behavior of Prestressed Concrete Beams With Web Reinforcement," Ph.D. Thesis, Department of Civil Engineering, University of Illinois at Urbana-Champaign, Urbana, IL, 1960, 295 pp.
10. Collins, M. P., Mitchell, D., Adebar, P. E., and Vecchio, F. J., "A General Shear Design Method," *ACI Structural Journal*, V. 93, No. 1, January-February 1996, pp. 36-45.

JOHN M. KULICKI,* SCOTT R. ESHENAUR† and ANDREW L. THOMAS‡

Modjeski and Masters, Inc. has reviewed the article titled "Shear Behavior of Full-Scale Prestressed Concrete Girders: Comparison Between AASHTO Specifications and LRFD Code" published in the PCI JOURNAL. This discussion will show the differences between the findings by the authors of the article and those of the writers of this discussion. Using the test data from the article, the results from this work show that the LRFD results are generally more conservative than the results obtained by use of the AASHTO method.

The authors stated that the LRFD method could be very conservative for some situations and very unconservative in other situations. The writers believe the LRFD values provided in the article do not properly reflect the correct use of the LRFD equations. The results presented in this discussion show that the LRFD method is only slightly more conservative than AASHTO for these test beam results, but has other advantages summarized herein.

This discussion is divided into four sections. The first section will provide a brief statement of the AASHTO and LRFD shear design specifications. The second section will show the test beam data taken (and assumed) from the article. The third section will provide sample calculations for both the AASHTO and LRFD methods. The last section will provide a comparison of the test results to the calculated values from the AASHTO and LRFD methods. Conclusions and recommendations are also provided.

SHEAR DESIGN METHODS

The AASHTO shear design method is based on the constant 45-degree truss analogy. The LRFD shear design method uses the modified compression field theory, which is based on a variable angle truss analogy. An outline of both shear design methods is provided in the article so it is not repeated in this discussion.

* President and Chief Engineer, Modjeski and Masters, Inc., Mechanicsburg, Pennsylvania.
† Associate, Modjeski and Masters, Inc., Mechanicsburg, Pennsylvania.
‡ Modjeski and Masters, Inc., Mechanicsburg, Pennsylvania.

BEAM TEST DATA FROM ARTICLE

This section provides the data from the article that is needed in the calculation of shear capacity of the test beams.

Fig. I provides the cross section of the AASHTO Type II beams with the deck slab. Table B provides the prestressing strand data which is the same within each group.

Fig. J shows the basic vertical shear reinforcement pattern for the 41 and 21 ft (12.5 and 6.4 m) beams. From the article, the basic vertical shear reinforcement that was designed using the AASHTO method is designated as the "R" series. Within each group, the shear reinforcement was varied. The last designation in the group name tells what type of shear reinforcement is in the beam as follows:

- 0R = no shear reinforcement
- R/2 = one-half of the basic vertical shear reinforcement "R"
- 3R/2 = one and a half times the basic vertical shear reinforcement "R"
- 2R = two times the basic vertical shear reinforcement "R"
- 3R = three times the basic vertical shear reinforcement "R"
- M = minimum specified in the AASHTO Specification

Fig. K provides the basic test setup of the test beams. Table C provides end tested, span length, shear span, shear reinforcement and concrete strength for each beam tested.

SAMPLE CALCULATIONS

Because test values are being compared to calculated values of a known cross section, this is not a design-type problem but a rating-type problem. Therefore, the design equations cannot be used directly. Sample calculations are given for both methods to show how both methods should be used in rating-type problems. Because this comparison is being made to failure test values, both load factors and resistance factors are taken as 1.0.

As shown below, the AASHTO method has fewer calculations than the LRFD method. However, the AASHTO method only checks the shear strength at the point of loading whereas the LRFD method checks three items: shear at

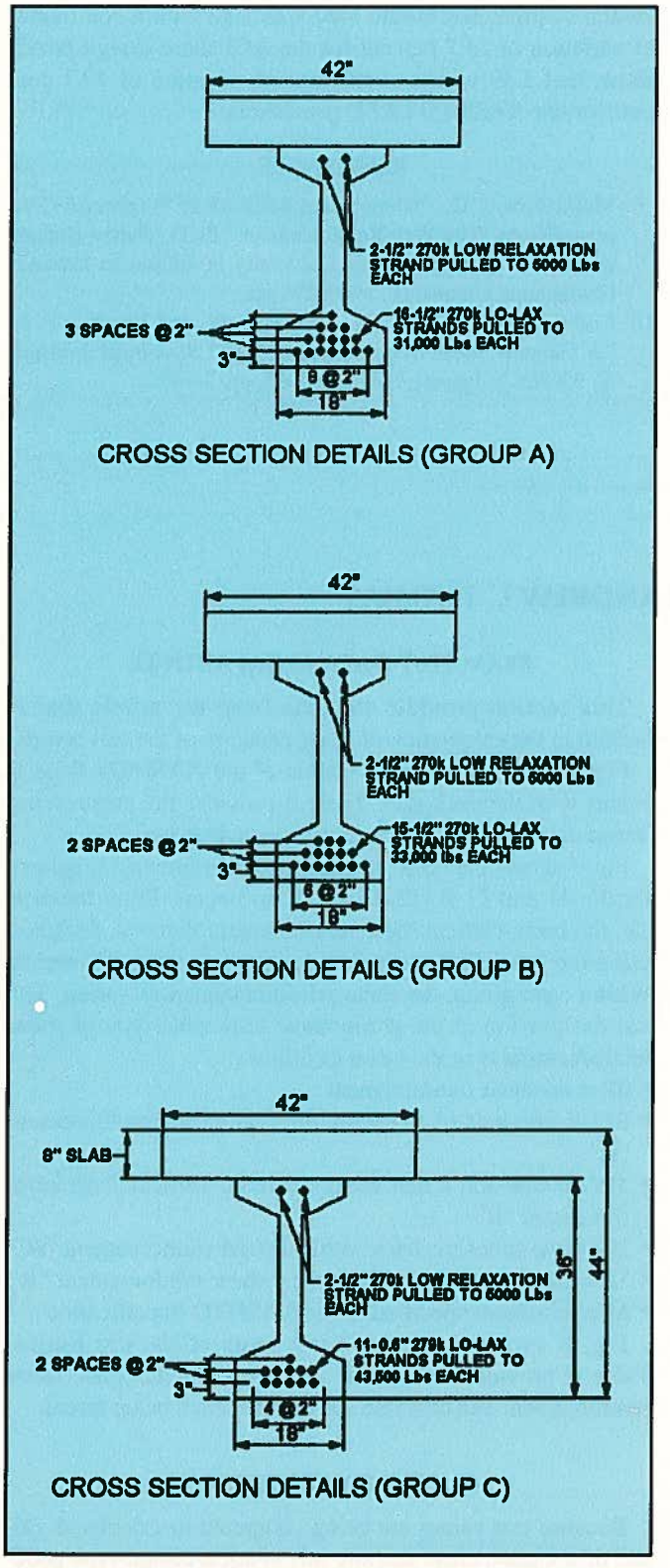

	Area (sq in.)	Moment of inertia (in.^{4})	y_{top} (in.)	y_{bott} (in.)
AASHTO Type II beam Non-composite	369	50,980	20.17	15.83
AASHTO Type II beam Composite with 42 × 8 in. deck	705	155,515	16.66	27.34

Fig. I. Test beam cross sections.

Table B. Prestressing strand data [270 ksi (1860 MPa), low-relaxation strand].

Group	Strand size (in.)	Strand area* (sq in.)	Number of strands†	Center of gravity from bottom flange* (in.)
A	0.5	0.153	16	4.75
B	0.5*S*	0.167	15	4.47
C	0.6	0.217	11	4.27

Note: 1 in. = 25.4 mm; 1 sq in. = 645.2 mm^2.
* Assumed or calculated data, not directly provided in PCI article.
† The two partially prestressed strands in the top flange are neglected.

the point of loading, longitudinal reinforcement at the point of loading and longitudinal reinforcement adjacent to the bearing. Because the equations for the shear strength include the applied load, the solution becomes an iterative process which converges to a value. In the AASHTO method, only V_{ci} includes the applied load and for this loading V_i/M_{max} is a constant ratio. However, in the LRFD method, all three checks show one iteration of the applied load to obtain a converged value.

In a design mode, the difference in calculations between the AASHTO and LRFD methods should not be as great because the designer would be selecting the amount of reinforcement needed and would not have to iterate the loading. Also, the longitudinal reinforcement at the bearing is checked once for a beam. It is not checked for the design of each section.

The transverse shear reinforcement is Grade 60. However, anecdotal information suggests that the actual yield strength, f_{sy}, is approximately 70 ksi (482 MPa). In order to replicate the test results, the calculations will use 70 ksi (482 MPa) for the shear reinforcement yield strength.

In the selection of shear area and spacing for calculations in this discussion, the area and spacing at the point of the test load was selected. However, a shear failure occurs on an inclined plane rather than a vertical one. Therefore, a more accurate representation of the shear reinforcement would have been an average area and spacing over the inclined plane rather than at the location of the test load. For beams that have the test load very close to a shear reinforcement transition, this change could have a noticeable effect on the shear capacity.

Although not used in these calculations, a further refinement for the LRFD method would be to move the critical section d_v back from the load instead of the section at the load. LRFD Article 5.8.3.2 explains that at the support, the critical section can be taken at distance d_v from the support. In these beams, the test load is applied at one stationary point, which is similar to the support condition and moving the critical section would be acceptable.

AASHTO METHOD CALCULATIONS FOR SHEAR CAPACITY OF TEST BEAM B1-00-R NORTH

$f_c' = 7.2$ ksi (49.6 MPa)
$L = 240$ in. (6.1 m)
$a = 60$ in. (1524 mm)

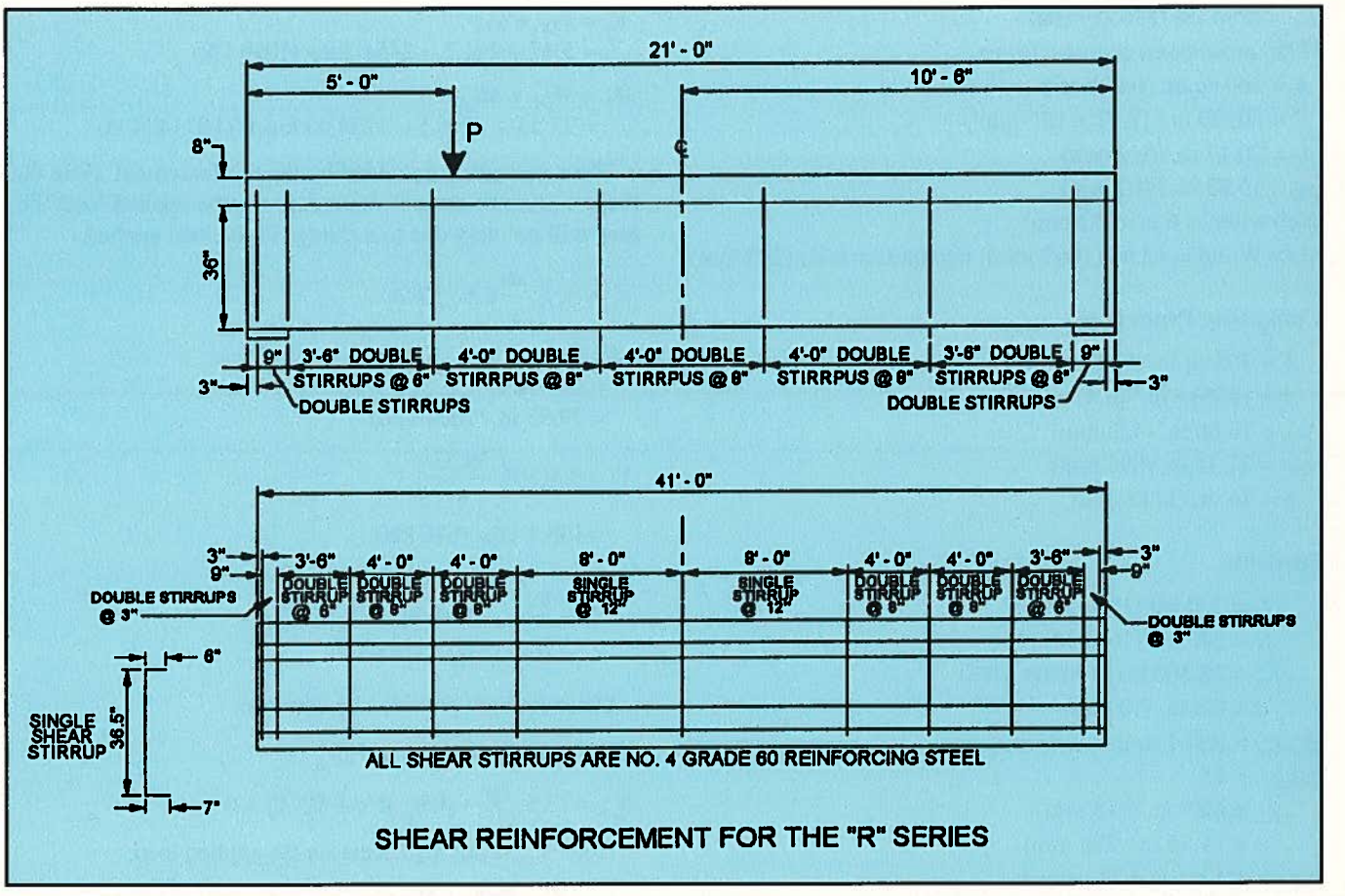

Fig. J. Shear reinforcement details.

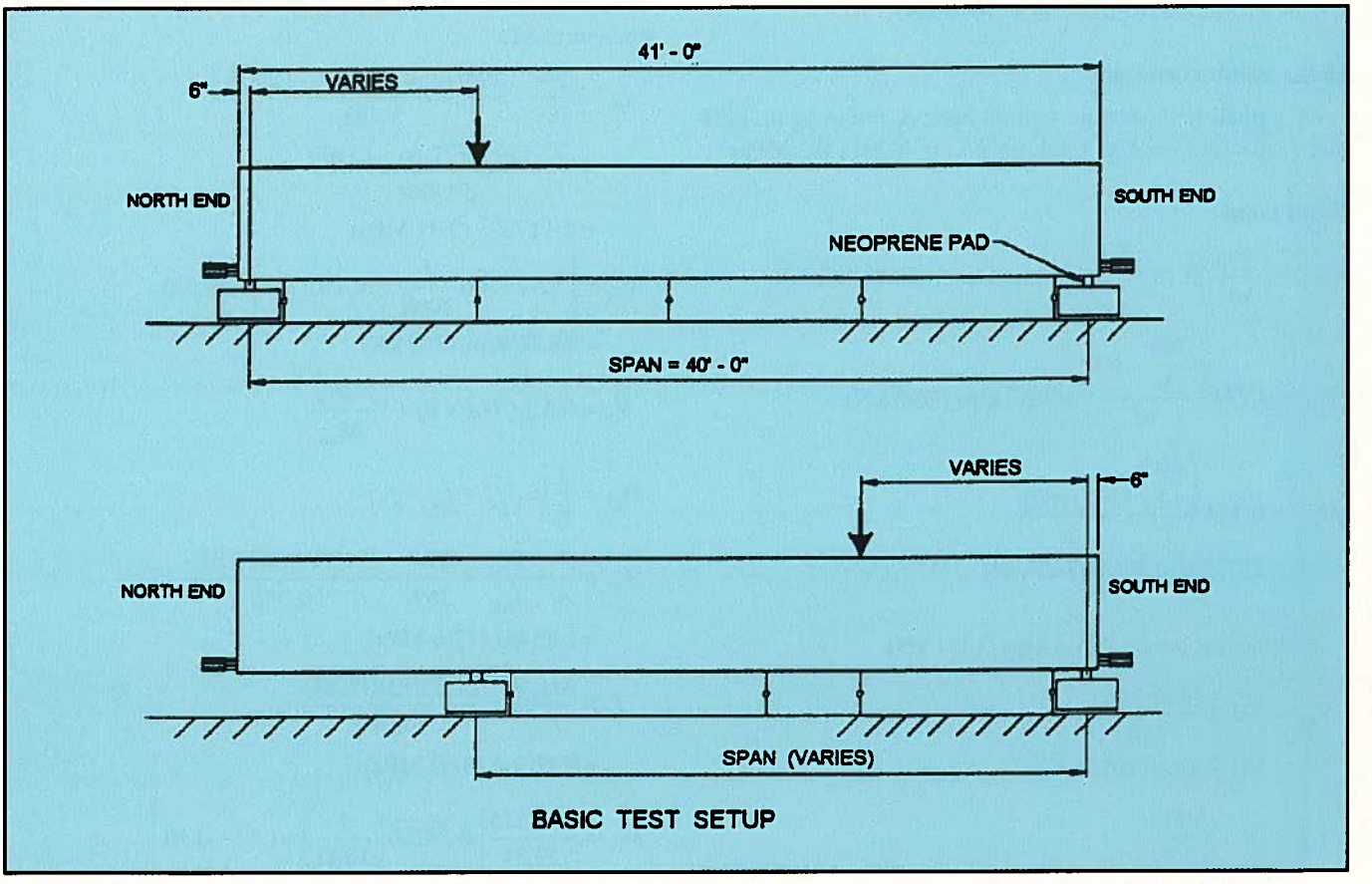

Fig. K. Basic test setup.

E_c = 4884 ksi (33675 MPa)
18/36 prestressed concrete beam
A = 369 sq in. (0.238 m²)
I = 50980 in.⁴ (2.12×10^{10} mm⁴)
y_T = 20.17 in. (512 mm)
y_B = 15.83 in. (402 mm)
Web width = 6 in. (152 mm)
Slab: Width = 42 in. (1067 mm); thickness = 8 in. (203 mm)

Composite Properties

A = 705 sq in. (0.454 m²)
I = 155515 in.⁴ (6.47×10^{10} mm⁴)
y_{TS} = 16.66 in. (423 mm)
y_{BC} = 27.34 in. (694 mm)
h = 44 in. (1118 mm)

Prestress

f_s = 270 ksi (1860 MPa)
f_y = 243 ksi (1675 MPa)
E_p = 28,500 ksi (196508 MPa)
d = 0.5 in. (13 mm)
A_{strand} = 0.167 sq in. (108 mm²)
$n_{strands}$ = 15
cgs = 4.47 in. (113 mm)
e = 11.36 in. (288 mm)
Prestress Losses = 27 percent
A_{ps} = 15(0.167) = 2.505 sq in. (1616 mm²)
Low-relaxation strands pulled to 33.8 kips (150 kN)
P = 147.75(2.505) = 370.1 kips (1646 kN)

Shear Reinforcement

At applied load section: two #4 bars: A_v = 0.4 sq in. (258 mm²); spacing, s = 8 in. (203 mm); f_{sy} = 70 ksi (482 MPa)

Dead Load

$$w_{DL} = \left(\frac{705}{144}\right)0.150 = 0.734 \text{ kips per ft (10.71 kN/m)}$$

$$V_{DL} = 0.734\frac{\left(\frac{240}{2} - 60\right)}{12} = 3.67 \text{ kips (16.3 kN)}$$

$$M_{DL} = 0.734\frac{\left(\frac{60}{12}\right)}{2}\frac{(240-60)}{12}$$
$$= 27.53 \text{ kip-ft (37.3 kN-m)}$$

Assume test load = 321.8 kips (1431 kN)

$$V_{LL} = 321.8\frac{(240-60)}{240}$$
$$= 241.3 \text{ kips (1073 kN)}$$

$$M_{LL} = 241.3\left(\frac{60}{12}\right)$$
$$= 1206.5 \text{ kip-ft (1636 kN-m)}$$

$$V_u = V_{DL} + V_{LL}$$
$$= 3.67 + 241.3 = 245.0 \text{ kips (1090 kN)}$$

$$M_u = M_{DL} + M_{LL}$$
$$= 27.53 + 1206.5 = 1234.03 \text{ kip-ft (1673 kN-m)}$$

Shear strength is provided by the reinforcement. Note that these equations are not dependent on the applied load, i.e., they will not vary due to a change in the load applied.

$$V_s = A_v f_{sy}\frac{d}{s} \le 8\sqrt{f_c'}b'd$$

$$d = h - cgs$$
$$= 44 - 4.47$$
$$= 39.53 \text{ in. (1004 mm)}$$

$$V_s = 0.4(70)\left(\frac{39.53}{8}\right)$$
$$= 138.4 \text{ kips (616 kN)}$$

$$V_{smax} = 8\sqrt{7200}\left(\frac{1}{1000}\right)(6)(39.53)$$
$$= 161.0 \text{ kips (716 kN)}$$

Shear strength provided by concrete:

V_c = minimum of V_{ci} or V_{cw}

$$V_{cw} = (3.5\sqrt{f_c'} + 0.3f_{pc})b'd + V_p;\ V_p = 0$$

Note: V_{cw} is not dependent on the applied load.

$$f_{pc} = \frac{P}{A} + \frac{Pey'}{I} - \frac{M_{DL}y'}{I}$$

P = 370.1(66/83) = 294 kips (1308 kN), adjusted for development length

$$f_{pc} = \frac{294}{369} - \frac{294(11.36)(27.34-15.83)}{50{,}980} + \frac{27.53(12)(27.34-15.83)}{50{,}980}$$
$$= 0.117 \text{ ksi (0.81 MPa)}$$

$$V_{cw} = \left[3.5\sqrt{7200}\frac{1}{1000} + 0.3(0.117)\right]6(39.53)$$
$$= 78.76 \text{ kips (350 kN)}$$

$$V_{ci} = 0.6\sqrt{f_c'}b'd + V_d + V_i\frac{M_{cr}}{M_{max}}$$

$$M_{cr} = \frac{I}{Y_t}\left(6\sqrt{f_c'} + f_{pe} - f_d\right)$$

$$f_{pe} = \frac{P}{A} + \frac{Pey}{I_{NC}} = \frac{294}{369} + \frac{294(11.36)(15.83)}{50{,}980}$$
$$= 1.83 \text{ ksi (12.6 MPa)}$$

$$f_d = \frac{M_{DL}y}{I_{NC}} = \frac{27.53(12)(15.83)}{50{,}980}$$
$$= 0.10 \text{ ksi (0.69 MPa)}$$

$$M_{cr} = \frac{155{,}515}{27.34}\left[6\sqrt{7200}\left(\frac{1}{1000}\right) + 1.83 - 0.10\right]$$
$$= 12{,}737 \text{ kip-in. (1439 kN-m)}$$

$$V_{ci} = 0.6\sqrt{7200}\left(\frac{1}{1000}\right)(6)39.53 + 3.67 + \frac{241.3(12737)}{1206.5(12)}$$

$$= 12.08 + 3.67 + 212.3$$

$$= 228.0 \text{ kips (1014 kN)}$$

Note: V_{ci} is dependent on the applied load. Therefore, the applied load will now be assumed to be 160 kips (712 kN) and V_{ci} will be recalculated.

$$V_{LL} = 160\left(\frac{240 - 60}{240}\right) = 120 \text{ kips (534 kN)}$$

$$M_{LL} = 120\left(\frac{60}{12}\right) = 600 \text{ kip - ft (814 kN - m)}$$

$$V_{ci} = 0.6\sqrt{7200}\left(\frac{1}{1000}\right)(6)39.53 + 3.67 + \frac{120(12,737)}{600(12)}$$

$$= 12.08 + 3.67 + 212.3$$

$$= 228.0 \text{ kips (1014 kN)}$$

This shows that although the applied load is changed, the ratio between the shear and moment do not change. This leads to V_{ci} being constant for this type of loading condition.

Table C. Test beam data.

Girder number	End	Span L (in.)	Shear span a (in.)	Shear reinforcement at test location		Concrete strength f_c* (psi)
				A_v* (sq in.)	s* (in.)	
A0-00-R	N	480	85	0.40	8	7000
A0-00-R	S	324	85	0.40	8	7000
A1-00-M	N	480	102	0.20	12	7000
A1-00-M	S	378	124	0.20	12	7000
A1-00-R/2	N	480	102	0.20	16	7000
A1-00-R/2	S	378	124	0.20	16	7000
A1-00-R	N	480	102	0.20	8	7000
A1-00-R	S	378	124	0.20	8	7000
A1-00-3R/2	N	480	102	0.60	16	7000
A1-00-3R/2	S	378	124	0.60	16	7000
A2-00-2R	N	480	102	0.40	8	6800
A2-00-2R	S	378	74	0.80	8	6800
A2-00-3R	N	480	102	0.60	8	6800
A2-00-3R	S	378	85	1.20	8	6800
A4-00-0R(1)	N	288	90	0.00	0	7000
A4-00-0R(1)	S	288	90	0.00	0	7000
A4-00-0R(2)	N	288	72	0.00	0	7000
A4-00-0R(2)	S	288	72	0.00	0	7000
B0-00-R	N	480	102	0.20	8	7000
B0-00-R	S	378	124	0.20	8	7000
B0-00-2R	N	480	102	0.40	8	7000
B0-00-2R	S	378	124	0.40	8	7000
B0-00-3R	N	480	102	0.60	8	7000
B0-00-3R	S	378	124	0.60	8	7000
B1-00-0R	N	240	60	0.00	0	7200
B1-00-0R	S	222	54	0.00	0	7200
B1-00-R	N	240	60	0.40	8	7200
B1-00-R	S	222	54	0.40	8	7200
B1-00-2R	N	240	60	0.80	8	7200
B1-00-2R	S	222	54	0.80	8	7200
B1-00-3R	N	240	60	1.20	8	7200
B1-00-3R	S	222	54	1.20	8	7200
B1-00-2R2	N	240	60	0.80	8	7200
B1-00-2R2	S	222	54	0.80	8	7200
C0-00-R	N	336	142	0.20	8	7000
C0-00-R	S	480	132	0.20	8	7000
C1-00-R	N	480	142	0.20	8	7000
C1-00-R	S	378	132	0.20	8	7000
C1-00-3R/2	N	480	132	0.60	16	7000
C1-00-3R/2	S	378	126	0.60	16	7000

Note: 1 in. = 25.4 mm; 1 sq in. = 645.2 mm²; 1 psi = 0.006895 MPa.
* Assumed data, not directly provided in PCI JOURNAL article.

$$V_{ci\,min} = 1.7\sqrt{f_c'}b'd$$
$$= 1.7\sqrt{7200}\left(\frac{1}{1000}\right)(6)(39.53)$$
$$= 34.2 \text{ kips (152 kN)}$$

For shear strength provided by the concrete V_{cw} controls:

V_{cw} = 78.8 kips (350 kN)

$V = V_s + V_{cw}$

= 138.4 + 78.8 = 217 kips (965 kN)

The shear capacity for this beam using the AASHTO method is 217 kips (965 kN).

LRFD METHOD CALCULATIONS FOR SHEAR CAPACITY OF TEST BEAM B1-00-R NORTH

Note: Given data same as AASHTO method.

Assume test load = 250 kips (1112 kN)

$$V_{LL} = 250\left(\frac{240-60}{240}\right) = 187.5 \text{ kips (834 kN)}$$

$$M_{LL} = 187.5\left(\frac{60}{12}\right) = 937.5 \text{ kip-ft (1271 kN-m)}$$

V_U = 3.7 + 187.5 = 191.2 kips (850 kN)

M_U = 27.5 + 937.5 = 965.0 kip-ft (1309 kN-m)

Check 1: Shear at Design Location (LRFD Article 5.8.3.3):

Shear Rating

$d_e = 44 - 4.47 = 39.53$ in. (1004 mm)

$0.9d_e = 0.9(39.53) = 35.58$ in. (903 mm)

$0.72h = 0.72(44) = 31.68$ in. (804 mm)

35.58 in. (903 mm) = minimum d_v

From LRFD Table C5.7.3.1.1-1: $k = 0.28$

$d_p \approx d_e$

$\beta_1 = 0.7$ for concrete with $f_c' = 7.0$ ksi (48.3 MPa)

$$C = \frac{A_{ps}f_{pu}}{\left(0.85f_c'\beta_1 b + \frac{kA_{ps}f_{pu}}{d_p}\right)}$$
$$= \frac{2.505(270)}{0.85(7.2)(0.7)(42) + \frac{0.28(2.505)(270)}{39.53}}$$
$$= 3.66 \text{ in. (93.0 mm)}$$

$$f_{ps} = f_{pu}\left(1 - \frac{kc}{d_p}\right)$$
$$= 270\left(1 - \frac{0.28(3.66)}{39.53}\right)$$
$$= 263.00 \text{ ksi (1813 MPa)}$$

$l_t = 60d_b = 60(0.5) = 30$ in. (762 mm)

$$l_d = \left(f_{ps} - \frac{2}{3}f_{pe}\right)d_b$$
$$= \left[263 - \frac{2}{3}(147.75)\right](0.5)$$
$$= 82.25 \text{ in. (2090 mm)}$$

Rating Design Section at 60 + 6 to end of beam = 66 in. (1676 mm)

f_{ps}^* can be assumed to vary from f_{pe} to f_{ps} between the transfer and development length:

$$f_{ps}^* = f_{pe} + \left(\frac{f_{ps} - f_{pe}}{l_d - l_t}\right)[(a+6) - l_t]$$
$$= 147.75 + \left(\frac{263 - 147.75}{82.25 - 30}\right)[(60+6) - 30]$$
$$= 227.16 \text{ ksi (1566 MPa)}$$

Percent of strands developed = 100(227.16/263)

= 86.4 percent

Reduced A_{ps} in the ε_x equation by 0.864

$$d_v = h - cgs - \frac{\beta_1 c}{2}$$
$$= 44 - 4.47 - \frac{0.7(3.66)}{2}$$
$$= 38.25 \text{ in. (971 mm)} > 35.58 \text{ in. (904 mm)}$$

Use d_v = 38.25 in. (971 mm):

$V_p = 0$

$$V = \frac{V_u - \phi V_p}{\phi b_v d_v} = \frac{191.2}{1.0(6)(38.25)}$$
$$= 0.833 \text{ ksi (5.74 MPa)}$$

$$\frac{v}{f_c'} = \frac{0.833}{7.2} = 0.116$$

$$f_{pc} = \frac{-P}{A} + \frac{(-Pe + M_{DL})e}{I}$$
$$= \frac{-370.1}{369} + \frac{[-370.1(11.36) + 27.5(12)](11.36)}{50{,}980}$$
$$= -1.866 \text{ ksi (-12.9 MPa)}$$

$$f_{po} = f_{pe} + \frac{f_{pc}E_p}{E_c}$$
$$= 147.75 + \left[\frac{1.866(28{,}500)}{4884}\right]$$
$$= 158.64 \text{ ksi (1093 MPa)}$$

Assume $\theta = 36$ degrees:

$$\varepsilon_x = \frac{\frac{M_u}{d_v} + 0.5N_u + 0.5V_u \cot\theta - A_{ps}f_{po}}{E_sA_s + E_pA_{ps}}$$
$$= \frac{\frac{965.0(12)}{38.25} + 0 + 0.5(191.2)\cot 36^\circ - [0.864(2.505)158.64]}{0 + 28{,}500[0.864(2.505)]}$$
$$= \frac{302.7 + 131.6 - 343.3}{61{,}683} = 1.475 \times 10^{-3}$$

Using linear interpolation of LRFD Table 5.8.3.4.2-1—> for $\theta = 36$ degrees and $v/f_c' = 0.125$, ε_x should equal 1.00×10^{-3}.

Assume $\theta = 36.8$ degrees.

$$\varepsilon_x = \frac{302.7 + 0.5(191.2)\cot 36.8 - 343.3}{61{,}683}$$

$$= 1.414 \times 10^{-3}$$

for $\theta = 36.8$ degrees ε_x should equal 1.4×10^{-3} (ok)

for $\theta = 36.8$ degrees and $v/f_c' = 0.125$: $\beta = 1.68$

$$V_c = 0.0316\beta\sqrt{f_c'}b_v d_v$$

$$= 0.0316(1.68)\sqrt{7.2}(6)(38.25)$$

$$= 32.7 \text{ kips (145 kN)}$$

$$V_s = \frac{A_v f_y d_v \cot\theta}{S}$$

$$= \frac{0.4(70)(38.25)\cot 36.8}{8}$$

$$= 178.9 \text{ kips (796 kN)}$$

Table D. Test results.

Girder number (1)	End (2)	L (in.) (3)	a (in.) (4)	Shear at first slip V_{slip} (kips) (5)	Test V (kips) (6)	Failure mode (7)
A0-00-R	N	480	85	259	313	Shear/Bond
A0-00-R	S	324	85	276	276	Shear
A1-00-M	N	480	102	129	141	Shear/Bond
A1-00-M	S	378	124	135	168	Shear/Bond
A1-00-R/2	N	480	102	136	166	Shear/Bond
A1-00-R/2	S	378	124	162	173	Shear/Bond
A1-00-R	N	480	102	144	210	Shear/Bond
A1-00-R	S	378	124	190	208	Flexure
A1-00-3R/2	N	480	102	161	207	Shear/Bond
A1-00-3R/2	S	378	124	185	230	Flexure
A2-00-2R	N	480	102	241	257	Flexure
A2-00-2R	S	378	74	282	357	Flexure
A2-00-3R	N	480	102	256	257	Flexure
A2-00-3R	S	378	85	273	312	Flexure
A4-00-0R(1)	N	288	90	84.8	93.9	Shear
A4-00-0R(1)	S	288	90	85.1	97.6	Shear
A4-00-0R(2)	N	288	72	100.5	100.5	Shear
A4-00-0R(2)	S	288	72	105.7	105.7	Shear
B0-00-R	N	480	102	185	220	Shear/Bond
B0-00-R	S	378	124	207	206	Shear
B0-00-2R	N	480	102	182	223	Flexure/Bond
B0-00-2R	S	378	124	195	216	Flexure
B0-00-3R	N	480	102	194	231	Flexure/Bond
B0-00-3R	S	378	124	216	236	Flexure
B1-00-0R	N	240	60	133	166	Shear/Bond
B1-00-0R	S	222	54	147	155	Shear/Bond
B1-00-R	N	240	60	228	245	Shear/Bond
B1-00-R	S	222	54	215	232	Shear/Bond
B1-00-2R	N	240	60	243	262	Shear/Bond
B1-00-2R	S	222	54	232	247	Shear/Bond
B1-00-3R	N	240	60	233	264	Shear/Bond
B1-00-3R	S	222	54	243	263	Shear/Bond
B1-00-2R2	N	240	60	238	268	Shear/Bond
B1-00-2R2	S	222	54	237	255	Shear/Bond
C0-00-R	N	336	142	176	176	Flexure
C0-00-R	S	480	132	180	180	Flexure
C1-00-R	N	480	142	177	177	Flexure
C1-00-R	S	378	132	196	196	Flexure
C1-00-3R/2	N	480	132	192	192	Flexure
C1-00-3R/2	S	378	126	202	202	Flexure

Note: 1 in. = 25.4 mm; 1 kip = 4.448 kN.

$V_n = V_c + V_s + V_p$
$= 32.7 + 178.9 + 0 = 211.6$ kips (941 kN)

Max $V_n = 0.25 d_v f'_c b_v = 0.25(38.25)(7.2)(6)$
$= 413.1$ kips (1837 kN) > 211.6 kips (940 kN) (ok)

$V_n > V_{applied} = 191$ kips (850 kN); therefore, increase assumed failure load.

Assume test load = 265.0 kips (1179 kN):

$$V_{LL} = 265.0\left(\frac{240-60}{240}\right) = 198.8 \text{ kips (884 kN)}$$

$$M_{LL} = 198.8\left(\frac{60}{12}\right) = 993.8 \text{ kip-ft (1347 kN-m)}$$

$V_u = 202.4$ kips (900 kN)

$M_u = 1021.3$ kip-ft (1385 kN-m)

$$v = \frac{202.4}{[1.0(6)(38.25)]} = 0.882$$

$$\frac{v}{f'_c} = \frac{0.882}{7.2} = 0.122$$

Assume $\theta = 37.5$ degrees:

$$\varepsilon_x = \frac{\frac{1021.3(12)}{38.25} + 0.5(202.4)\cot 37.5 - [0.864(2.505)](158.64)}{28,500(0.864)(2.505)}$$

$$= \frac{302.4 + 131.9 - 343.3}{61,683}$$

$$= 1.767 \times 10^{-3}$$

for $\theta = 37.5$ degrees and $v/f'_c = 0.125$:
ε_x should equal 1.750×10^{-3} for $\theta = 37.5$ degrees and $v/f'_c = 0.125$: $\beta = 1.48$

$V_c = 0.0316(1.48)\sqrt{7.2}(6)(38.25) = 28.8$ kips (128 kN)

$$V_s = \frac{0.4(70)(38.25)\cot 37.5}{8} = 174.4 \text{ kips (776 kN)}$$

$V_n = 28.8 + 174.4 + 0 = 203$ kips (903 kN)

$V_n = V_{applied} = V_u$; therefore, the shear capacity at this location is 202 kips (898 kN).

Check 2: Longitudinal Reinforcement (LRFD Article 5.8.3.5a)

At the edge of the bearing:

Longitudinal Tensile Resistance > $(V_n - 0.5V_s - V_p)\cot\theta$. In our case, prestressing strands are the only resistance and $V_p = 0$. Therefore, $A_{ps}f_{ps} > (V_n - 0.5V_s)\cot\theta$

At the bearing:

$$\max V_n = \frac{A_{ps}f_{ps}}{\cot\theta} + 0.5V_s$$

V_s is based on double stirrups at 6 in. (152 mm) and the assumption that θ at the bearing = θ at the design section.

f^*_{ps} = prestressing force reduced for lack of development bearing length = 12 in. < 30 in. = l_t

$$f^*_{ps} = f_{pe}\left(\frac{12}{30}\right) = 59.1 \text{ ksi (407 MPa)}$$

$\max V_s = \max V_n - V_c$
$= 413.1 - 28.8$
$= 384.3$ kips (1709 kN)
$V_s = 0.4(70)(38.25)\cot 37.5/6$
$= 232.6$ kips (1034 kN)

$$\max V_n = \frac{2.505(59.1)}{\cot 37.5} + 0.5(232.6)$$

$= 229$ kips (1018 kN) > $V_u = 202$ kips (898 kN)

Therefore, longitudinal reinforcement does not control shear rating.

Check 3: Max V_n based on Longitudinal Reinforcement at "a" Section (LRFD Article 5.8.3.5b)

$$A_{ps}f_{ps} \geq \frac{M_u}{d_v} + \left[\left(V_n - 0.5V_s\right)\cot\theta\right]$$

Max V_n is a function of the loading. Therefore, we must adjust the load until it converges to Max V_n (similar to previous iterations).

Assume Test Load = 310.0 kips (1379 kN)

$V_{LL} = 232.5$ kips (1034 kN)
$M_{LL} = 1162.5$ kip-ft (1576 kN-m)
$V_u = 236.2$ kips (1051 kN)
$M_u = 1190.0$ kip-ft (1614 kN-m)

$$v = \frac{236.2}{1.0(6)(38.25)} = 1.029 \text{ ksi (7.09 MPa)}$$

$v/f'_c = 1.029/7.2 = 0.143$. Conservative to use $v/f'_c = 0.150$

Try $\theta = 37.0$ degrees (ε_x should be $\geq 2 \times 10^{-3}$):

$$\varepsilon_x = \frac{\frac{1190(12)}{38.25} + 0.5(236.2)\cot 37.0 - [2.505(0.864)](158.64)}{2.505(0.864)28,500}$$

$$= \frac{373.3 + 156.7 - 343.3}{61,683}$$

$= 3.03 \times 10^{-3} > 2 \times 10^{-3}$ ok

For $\theta = 37.0$ degrees and $v/f'_c = 0.150$ —> $\beta = 1.24$

$V_s = 0.4(70)(38.25)\cot 37.0/8$
$= 177.7$ kips (790 kN)

$$\max V_n = \frac{\left(A_{ps}f^*_{ps} - \frac{M_u}{d_v}\right)}{\cot\theta} + 0.5V_s$$

$f^*_{ps} = 227.16$ ksi (1566 MPa) (calculated in Check 1)

$$\max V_n = \frac{\left[2.505(227.16) - \frac{1190(12)}{38.25}\right]}{\cot 37.0} + 0.5(177.7)$$

$= 236.3$ kips (1050 kN)

$V_n = V_u$, therefore, max $V_n = 236$ kips (1050 kN) > 202 kips (898 kN) — Does not control.

Table E. Comparison of test results to calculated values for Groups A, B and C.

Girder number (1)	End (2)	L (in.) (3)	a (in.) (4)	Test V (kips) (5)	Shear capacity per Shahawy article				Shear capacity based on Test V						
					AASHTO		LRFD		AASHTO		LRFD article				
					(6)	(5)/(6) (7)	(8)	(5)/(8) (9)	(10)	(5)/(10) (11)	5.8.3.3 (12)	5.8.3.5a (13)	5.8.3.5b (14)	Controlling (15)	(5)/(15) (16)
A0-00-R	N	480	85	313	230	1.36	201	1.56	228	1.37	196	231	212	196	1.60
A0-00-R	S	324	85	276	230	1.20	201	1.37	222	1.24	196	229	212	196	1.41
A1-00-M	N	480	102	141	130	1.08	67	2.10	139	1.01	121	126	170	121	1.17
A1-00-M	S	378	124	168	119	1.41	52	3.23	136	1.24	110	134	148	110	1.53
A1-00-R/2	N	480	102	166	143	1.16	84	1.98	128	1.30	115	122	168	115	1.44
A1-00-R/2	S	378	124	173	129	1.34	65	2.66	124	1.40	122	144	151	122	1.42
A1-00-R	N	480	102	210	202	1.04	146	1.44	162	1.30	135	231	174	135	1.56
A1-00-R	S	378	124	208	164	1.27	100	2.08	159	1.31	122	229	151	122	1.70
A1-00-3R/2	N	480	102	207	200	1.04	154	1.34	196	1.06	155	286	181	155	1.34
A1-00-3R/2	S	378	124	230	195	1.18	144	1.60	193	1.19	151	284	157	151	1.52
A2-00-2R	N	480	102	257	264	0.97	233	1.10	230	1.12	196	309	188	188	1.37
A2-00-2R	S	378	74	357	274	1.30	390	0.92	239	1.49	350	314	266	266	1.34
A2-00-3R	N	480	102	257	272	0.94	343	0.75	248	1.04	295	304	202	202	1.27
A2-00-3R	S	378	85	312	270	1.16	408	0.76	241	1.29	410	324	251	251	1.24
A4-00-0R(1)	N	288	90	93.9	101	0.93	43	2.18	83	1.13	97	98	226	97	0.97
A4-00-0R(1)	S	288	90	97.6	101	0.97	43	2.27	83	1.18	97	98	226	97	1.01
A4-00-0R(2)	N	288	72	100.5	96	1.05	80	1.26	81	1.24	101	94	265	94	1.07
A4-00-0R(2)	S	288	72	105.7	96	1.10	80	1.32	81	1.30	101	94	265	94	1.12
B0-00-R	N	480	102	220	194	1.13	147	1.50	162	1.36	136	233	179	136	1.62
B0-00-R	S	378	124	206	161	1.28	101	2.04	158	1.30	123	231	156	123	1.67
B0-00-2R	N	480	102	223	265	0.84	235	0.95	231	0.97	197	306	194	194	1.15
B0-00-2R	S	378	124	216	222	0.97	174	1.24	227	0.95	197	304	167	167	1.29
B0-00-3R	N	480	102	231	279	0.83	345	0.67	251	0.92	296	300	206	206	1.12
B0-00-3R	S	378	124	236	272	0.87	254	0.93	248	0.95	296	299	179	179	1.32
B1-00-0R	N	240	60	166	90	1.84	105	1.58	79	2.10	102	95	281	95	1.75
B1-00-0R	S	222	54	155	88	1.76	111	1.40	77	2.01	102	96	287	96	1.61
B1-00-R	N	240	60	245	212	1.16	271	0.90	217	1.13	202	230	236	202	1.21
B1-00-R	S	222	54	232	210	1.10	271	0.86	216	1.07	203	229	237	203	1.14
B1-00-2R	N	240	60	262	268	0.98	436	0.60	240	1.09	353	315	279	279	0.94
B1-00-2R	S	222	54	247	266	0.93	436	0.57	238	1.04	353	315	282	282	0.88
B1-00-3R	N	240	60	264	268	0.99	436	0.61	240	1.10	413	325	283	283	0.93
B1-00-3R	S	222	54	263	266	0.99	436	0.60	238	1.11	413	325	287	287	0.92
B1-00-2R2	N	240	60	268	268	1.00	436	0.61	240	1.12	353	315	278	278	0.96
B1-00-2R2	S	222	54	255	266	0.96	436	0.58	238	1.07	353	315	282	282	0.90
C0-00-R	N	336	142	176	147	1.20	86	2.05	155	1.14	112	206	135	112	1.57
C0-00-R	S	480	132	180	160	1.13	102	1.76	165	1.09	117	207	143	117	1.54
C1-00-R	N	480	142	177	147	1.20	86	2.06	166	1.07	113	207	135	113	1.57
C1-00-R	S	378	132	196	160	1.23	102	1.92	158	1.24	116	206	143	116	1.69
C1-00-3R/2	N	480	132	192	197	0.97	146	1.32	199	0.96	153	263	148	148	1.30
C1-00-3R/2	S	378	126	202	198	1.02	146	1.38	192	1.05	153	262	154	153	1.32

Notes: Assumptions used in the calculations for the PCI shear capacity are unknown. LRFD Article 5.8.3.3 calculates the shear capacity based on the shear stirrups at the loading point. LRFD Article 5.8.3.5a calculates the shear capacity based on the longitudinal reinforcement at edge of bearing. LRFD Article 5.8.3.5b calculates the shear capacity based on the longitudinal reinforcement at the loading point.

Table F. Statistical comparison of ratio of test shear to predicted values.

Series	Function	Per Shahawy article		Based on Test V	
		AASHTO	LRFD	AASHTO	LRFD
A	Average	1.14	1.66	1.23	1.34
	STD	0.147	0.650	0.125	0.204
	Max	1.41	3.23	1.49	1.70
	Min	0.93	0.75	1.01	0.97
B	Average	1.10	0.98	1.21	1.21
	STD	0.289	0.433	0.342	0.293
	Max	1.84	2.04	2.10	1.75
	Min	0.83	0.57	0.92	0.88
C	Average	1.12	1.75	1.09	1.50
	STD	0.096	0.299	0.084	0.142
	Max	1.23	2.06	1.24	1.69
	Min	0.97	1.32	0.96	1.30
Total	Average	1.12	1.40	1.20	1.31
	STD	0.212	0.632	0.239	0.256
	Max	1.84	3.23	2.10	1.75
	Min	0.83	0.57	0.92	0.88

The shear capacity for this beam using the LRFD method is 202 kips (898 kN).

COMPARISON OF RESULTS

Table D provides the test results of shear at first slip, shear at failure and the failure mode of the beam. This information is taken directly from the article.

Table E provides the shear at failure compared with the calculated shear resistance for the AASHTO method and LRFD method, using the results from the article and this discussion for the three groups of beams. This table shows that the LRFD values based on this discussion are much different than the LRFD values from the article. However, the AASHTO values calculated in either the article or this discussion do not vary nearly as much. Because there were no sample calculations provided in the article, the reasons for the differences in the calculated values between the article and this discussion are not readily apparent.

Table F provides a statistical comparison of the ratio of test shear to predicted values. The average, maximum and minimum ratio and the standard deviation of the ratios are shown. When looking at the results from the article, the LRFD values are clearly more variable than the AASHTO results. However, when comparing values calculated from this discussion, this table shows that the AASHTO values are only slightly better than the LRFD values in predicting the failure value.

Based on values calculated from this discussion, Fig. L provides a graph of the ratio of the test shear divided by the predicted shear vs. shear reinforcement ratio.

CONCLUSIONS AND RECOMMENDATIONS

Based on the results of this article, Table F shows that the LRFD method is more conservative than the AASHTO method for the beams tested. This is the opposite of the authors' conclusion. Sample calculations are provided herein so that readers can review how the methods are to be used. The article does not provide sample calculations or detailed information on how values where calculated, so no comments on these important issues can be provided by the writers. However, the writers believe that the LRFD method was not applied correctly in the article.

The beams selected for this study are in the short span range, particularly the 21 ft (6.4 m) beams. In order to provide a more objective view of the LRFD and AASHTO

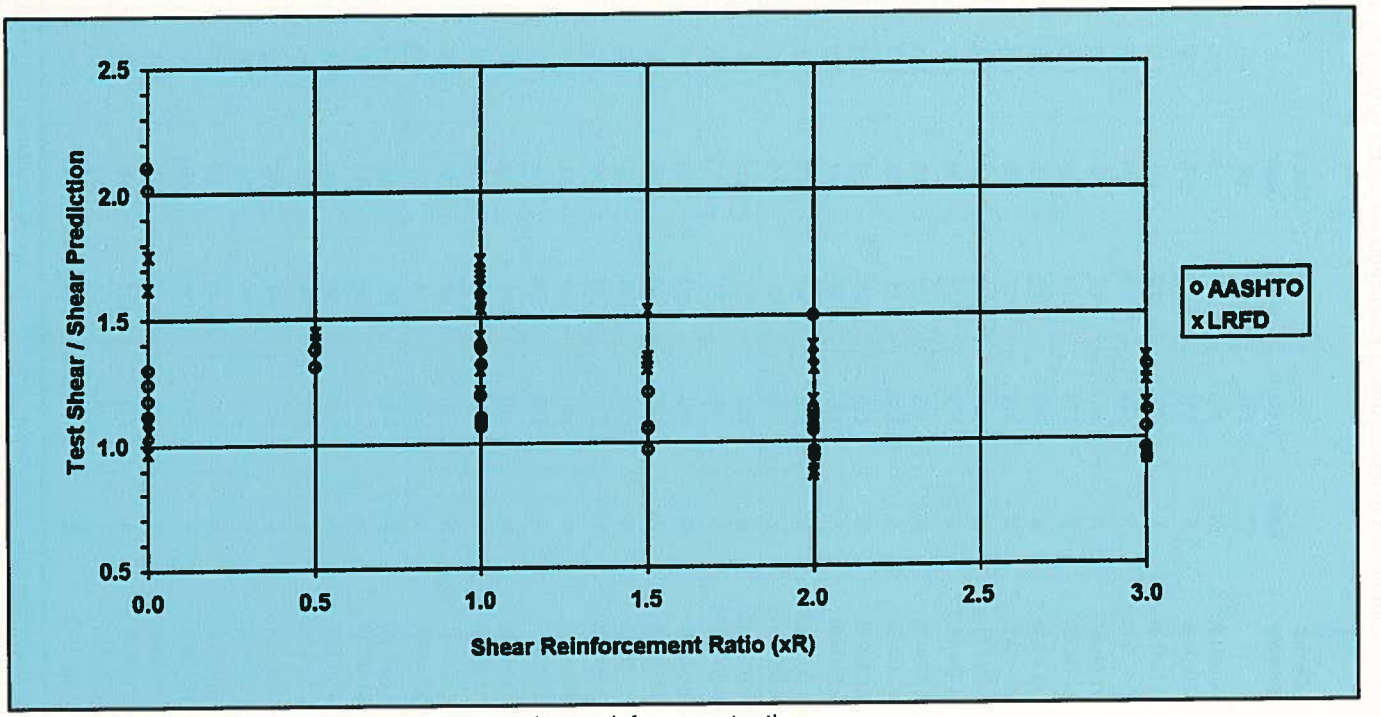

Fig. L. Ratio of test shear to predicted shear vs. shear reinforcement ratio.

LRFD methods, a variety of span lengths and beam sizes should be tested and compared. Also, some beams should be tested which have shear reinforcement that is designed based on the LRFD method.

The modified compression field theory was selected for use in the AASHTO LRFD Bridge Design Specifications after a review of several possible approaches to shear design. This method was selected because it represented a rational approach with few special case exceptions. In fact, because it deals with a basic phenomonological model, it represents a unified approach to shear design for plain, reinforced, partially prestressed and fully prestressed concrete components resisting any combination of shear, moment and axial thrust.

This unification of design would have been considered worthwhile, even if the statistics of comparisons to test results were somewhat less compelling than that of a series of special case equations for various types of concrete components. In fact, a study[10] of 528 test results showed the modified compression field theory to be slightly safer but much more uniform than the ACI or AASHTO Standard Specifications.*

* This is the same Ref. 10 that was cited in the previous discussion.

REFERENCE

10. Collins, M. P., Mitchell, D., Adebar, P. E., and Vecchio, F. J., "A General Shear Design Method," *ACI Structural Journal*, V. 93, No. 1, January-February 1996, pp. 36-45.

AUTHORS' CLOSURE by MOHSEN A. SHAHAWY* and BARRINGTON deV BATCHELOR†

The authors thank Dr. Kulicki et al. and Professor Collins for providing such exhaustive discussions. Dr. Kulicki and Professor Collins were heavily involved in the development of the LRFD provisions and that is why it is particularly welcome to have these discussions. Professor Collins is known to be a strong proponent of the LRFD shear design method. On the surface, both discussions are critical of the authors' findings. However, the authors will show that in fact these discussions strongly reinforce the authors' findings. The point made in Mr. Bassi's discussion is important and should be noted. Mr. Bassi was one of the pioneers involved in the development of the Concrete Structures Section of the Ontario Highway Bridge Code.

The authors' calculations presented in the PCI JOURNAL paper are based on factored design loads (dead and live) and specified material strengths, while the calculations of Dr. Kulicki et al. are based on test loads and actual material strengths, i.e., a rating check on the girder against test results. This may explain some of the differences between the separate sets of calculations. It is important to emphasize that the main objective of the authors' investigation was to compare the predicted shear strength along the girder based on AASHTO provisions with actual test values.

The comprehensive series of tests reported in the paper were planned and started before the draft LRFD Code appeared and were intended to investigate many other issues besides shear behavior of prestressed concrete girders. The girders were designed and detailed in accordance with the 1989 AASHTO provisions, which contain no specific requirement for longitudinal reinforcement at the end zones of prestressed concrete girders where congestion usually presents a serious problem in practice.

In the authors' study, the 1989 AASHTO Code was used to arrive at an appropriate design (i.e., R series). The 1994 LRFD requirements for longitudinal reinforcement were checked for this type of girder and no such reinforcement was required, as can also be seen in the worked example presented by Dr. Kulicki et al. In all other girders in the study (i.e., M, R/2, 3R/2, 2R and 3R), the percentage of the transverse shear reinforcement was varied, and in many cases exceeded the upper limits specified by both codes. The purpose of the variation was to study the effect on the girder behavior and strand slippage in comparison with a standard design (i.e., R series). No supplementary longitudinal reinforcement was provided in these girders because it was considered beyond the scope of the investigation.

For girders of the 2R and 3R series, the check for longitudinal reinforcement was not carried out in the original calculations. It is agreed that this check would have affected the results, as shown in the calculation by Dr. Kulicki et al. Despite this, Fig. L and Table F of the discussion by Dr. Kulicki et al. show that the 1989 AASHTO Code provides better predictions than the LRFD Code.

In order to compare the results by Dr. Kulicki et al. with those of the authors, the calculations were revised using the same assumptions stated by Dr. Kulicki et al., i.e., actual concrete strength, f_y = 70 ksi (483 MPa), prestress loss = 27 percent and ϕ =1.0 for all the R series girders. In this comparison, all the other non-standard girders were eliminated because they did not meet standard design requirements of both codes. Table G shows a comparison of the authors' calculations and those of Dr. Kulicki et al. as well as the corresponding results extracted from Table A of Professor Collins' discussion.

It is interesting to observe that the authors' calculations give almost identical results as those obtained by Dr. Kulicki et al. for both the AASHTO and LRFD Codes. However, the results presented by Professor Collins for the LRFD Code only are very different from those of Dr. Kulicki et al. and the authors. This raises a question as to whether Professor Collins' calculations are correct, or even

* Director, Structural Research Center, Florida Department of Transportation, Tallahassee, Florida.

† Professor of Civil Engineering, Queen's University, Kingston, Ontario, Canada.

Table G. Comparison of test results for R series girders.

Girder number	Test load (kips)	Test load/1989 AASHTO		Test load/LRFD		
		Authors	Kulicki et al.	Authors	Kulicki et al.	Collins
B0-00-R(N)	220	1.36	1.36	1.66	1.62	1.06
B0-00-R(S)	206	1.30	1.30	1.67	1.67	1.11
B1-00-R(N)	245	1.12	1.13	1.21	1.21	1.16
B1-00-R(S)	232	1.07	1.07	1.14	1.14	1.10
A0-00-R(N)	313	1.37	1.37	1.60	1.60	1.50
A0-00-R(S)	276	1.25	1.24	1.41	1.41	1.33
A1-00-R(N)	210	1.30	1.30	1.59	1.56	1.01
A1-00-R(S)	208	1.31	1.31	1.71	1.70	1.12
C0-00-R(N)	176	1.13	1.14	1.59	1.57	1.11
C0-00-R(S)	180	1.09	1.04	1.57	1.54	1.05
C1-00-R(N)	177	1.07	1.07	1.60	1.57	1.11
C1-00-R(S)	196	1.24	1.24	1.68	1.69	1.14
	Average	**1.22**	**1.21**	**1.54**	**1.52**	**1.15**

Note: 1 kip = 4.448 kN.

a more important concern as to whether there exists ambiguity in the LRFD Code provisions which can lead to different interpretations. It is clear that, as stated in the original paper, the 1989 AASHTO provisions give much better predictions of shear strength than the LRFD Code.

In their comparison of results, Dr. Kulicki et al. have concluded that the LRFD values are more variable than those based on the AASHTO Code. This again poses the question as to which method is more reliable.

Dr. Kulicki et al., in their section dealing with conclusions and recommendations, imply that the LRFD method is "slightly" more conservative than the AASHTO method. Table G shows that using calculations by the authors or by Dr. Kulicki et al., the LRFD Code yields predictions that are on the average 52 percent higher than the test results. In comparison, the predictions by the 1989 AASHTO Code are only 21 percent higher, which supports the authors' original findings.

The authors support the opinion of Dr. Kulicki et al. that a broader investigation of shear strength is required with the important shear parameters varied in order to check the two sets of code provisions exhaustively. The authors' work is a start and has raised some important questions. The authors also agree with Dr. Kulicki et al. regarding the rational approach of the modified compression field theory to shear design. This was clearly stated in the authors' paper, which also added that refinement of the method is necessary. The authors still maintain this opinion.

Professor Collins raises some issues that are only peripherally related to the authors' findings. As stated in the original paper and above, the main objective of the study is testing a girder to failure and applying both design codes to evaluate the predicted shear capacity. As long as the predicted shear capacity at a particular section by both codes is compared to the test shear capacity at the same section, and the same load configuration is used, the method of testing is immaterial. Professor Collins states that he would have loaded the girder with nine jacks. It is the opinion of the authors that this would not make any difference in a capacity comparison. Note that in Professor Collins' Fig. E at the loading point of 8 ft 5 in. (2565 mm) from the left support, the ratio M/V just to the left of the load point is of the same order as that in our paper.

In view of the large number of shear tests envisioned with full-scale specimens, the decision was made at the outset to use point loads in the shear tests. Because the LRFD and the 1989 AASHTO provisions are used to check the strength of a section for the same loading case, this does not constitute a compromise, as implied by Professor Collins. The literature is full of examples of the use of this simple testing approach.

Professor Collins states that the 1989 AASHTO Specifications or the 1995 ACI Code requires more work than doing the same task with the 1994 AASHTO LRFD provisions, which is incorrect as illustrated in the example provided by Dr. Kulicki et al. One can clearly judge, from this example, the high level of calculations required by the LRFD Code compared to the 1989 AASHTO Specifications. It would be interesting to hear comments from practicing engineers as to the amount of work involved in using the LRFD method.

Professor Collins states that the shear design procedure of the AASHTO LRFD Specifications were formulated for design and are less convenient in predicting the shear strength of a given member under given loading. He also adds that the procedure can be misinterpreted to produce unsatisfactory results. The statement poses a serious question regarding the rating of existing structures and failure analysis. Is there a need for a convenient method for this purpose? It should be emphasized that design and analysis are two sides of the same coin.

Professor Collins should be reminded that there exist many thousands of bridge members that have been successfully designed for shear without any reported failures before the advent of the LRFD Code. The modified compression field theory, or any other theory, is not perfect and usually requires refinement and modification with time and use. He should also be reminded that some shear provisions of the

LRFD Code are really empirical, and may have to be modified in the light of actual tests. Note that this was the fate of the original compression field theory. There is, therefore, no point in shooting the messenger if the message does not entirely endorse his theory. The authors have stressed the usefulness of the rational approach of the LRFD provisions, but have also pointed out that the 1989 AASHTO provisions yield extremely accurate results, as illustrated in Table G. The authors' findings are also supported by the results of Dr. Kulicki et al.

As shown in Table G and stated earlier, Professor Collins' results do not compare favorably with either the authors or Dr. Kulicki et al., which are in reasonably close agreement. In calculating shear reinforcement requirements with the LRFD provisions, Professor Collins should also have designed the end portions of the girders without longitudinal reinforcement as detailed in the paper and not with the four #5 U-bars. It is agreed that the use of such bars would be beneficial, regardless of the design method used, but alternate arrangements could include the use of end anchors to a small number of the strands — an idea which is under study by the first author. Note that the calculations by Dr. Kulicki et al. show that end longitudinal reinforcement is not required in the R series, as was stated in our paper.

It is, therefore, inappropriate for Professor Collins to introduce the use of this longitudinal reinforcement in comparing the shear reinforcement requirements for the girders using both the LRFD and 1989 AASHTO provisions. One could say that this constitutes a serious flaw in logic and is tantamount to comparing apples and oranges.

Dr. Kulicki determines the shear strength of Girder A1-00-R(S) to be 112 kips (498 kN) vs. 100 kips (445 kN) in the original paper. Professor Collins calculates the shear strength for the same girder to be 207 kips (921 kN) — nearly twice the other predictions. Is there ambiguity in the method such that separate calculations of shear strength give vastly different answers? This divergence alone calls into question the plot in Fig. G of Professor Collins' discussion. How reliable is the information in the figure? The calculations by Dr. Kulicki et al. give trends similar to those by the authors, while Fig. G of Professor Collins' discussion gives a much closer comparison to test results. Is there some basic inconsistency in the LRFD provisions such that only Professor Collins can obtain such good agreement with his theory while others cannot?

The failures of the 0R series (no shear reinforcement) at first cracking are treated too lightly by Professor Collins in the discussion of V_c. Certainly, the first shear cracking strength of the member without stirrups would represent a possible high limit of V_c after which a redistribution takes place in the form of other mechanisms that will be developed in a cracked member reinforced for shear. The calculation of V_c is surely one of the most empirical aspects of the LRFD provisions. Has Professor Collins generated any tests to check the LRFD Specifications for V_c? If so, it would have been helpful if he had presented the findings in his discussion.

CONCLUDING REMARKS

The authors' response confirms their previous findings that the 1989 AASHTO Specifications provide a much closer comparison to the test results than does the LRFD Code.

The conflicting results from the discussors who were heavily involved in the development of the shear provisions in the LRFD Code reinforce the authors' previously stated opinion that further refinements are required.

If, as stated by Professor Collins, the authors misinterpreted the LRFD Code, do the calculations by Dr. Kulicki et al. also reflect misinterpretation? Is this an indication that a close examination of the LRFD shear provisions is warranted as stated in our paper, especially for use by practicing engineers as opposed to researchers?